Cognitive Radio Network Tomography

Chung-Kai Yu, *Member, IEEE*, Kwang-Cheng Chen, *Fellow, IEEE*, and Shin-Ming Cheng, *Member, IEEE*

***Abstract*—The cognitive radio network (CRN), as a promising technique in future wireless communication networks, shall execute some critical functionalities to enhance existing wireless networks, such as network reconfigurability to adaptively select networks (e.g., in IEEE P1900.4 and ETSI-RSS), spectrum opportunity utilization for transmissions over opportunistic links to enhance spectrum efficiency (e.g., in IEEE 802.22), and further cooperative relays among cognitive radios (CRs) and nodes of coexisting multiradio systems, including heterogeneous primary systems. To support multilink operations and networking functions in CRN, traditional spectrum sensing is not enough, and we thus develop CRN tomography to meet the general needs of CRN operations at both the link and network levels. Borrowing the concept from medical/Internet tomography via statistical inferring, we establish the framework and methodology of CRN tomography that can be passive monitoring or active probing defined over link- or network-level parameter inference. Generally speaking, conventional CR spectrum-sensing techniques belong to the category of the passive link-level monitoring. Multiple-system sensing and identification can be considered as a sort of passive network-level CRN tomography. We further propose active link-level CRN tomography by examining the radio resource for transmissions. Finally, CRN tomography using active network-level probing is illustrated by the estimation of successful packet-transmission probability in network operations. This paper initiates explorations of CRN tomography obtaining the required parameters at the link and network levels for successful CRN operations.**

***Index Terms*—Cognitive radio networks (CRNs), multiple-system sensing, network tomography, radio-resource sensing, spectrum sensing, successful transmission probability estimation.**

I. Introduction

A. Cognitive Radio Network (CRN)

THE cognitive radio (CR) technology, which was a term first coined by Mitola [1], has attracted tremendous attention for the past decade in wireless communications due to its potential of improving the spectrum-scarcity problem invoked by current static spectrum-assignment policy [2]. Generally speaking, in conventional development of CR technology, one common approach is the opportunistic spectrum access (OSA, such as [3]–[7]), which allows CR nodes to search and exploit the spectrum opportunities without causing interference to primary system (PS) nodes. Numerous available spectrum-sharing techniques of OSA have been proposed to provide CR nodes with the capability of sharing the wireless channel(s) with PS nodes in an opportunistic way with underlay, overlay, or interweave structures [8]–[10]. Under this scenario, CR and its spectrum sensing is functioning at the link level (transmitter–receiver) for opportunistic radio transmission, i.e., node-to-node transmissions among neighboring nodes using OSA, to achieve better spectrum efficiency from the throughput of secondary system(s) (CR nodes). In recent research, such as [10], despite establishing the CR opportunistic link transmission, the development of technologies to network CR nodes operating over the entire coexisting multiradio environment to provide the networking "macroscale diversity," which is known as CRN to enhance network efficiency/throughput, given spectrum bandwidth as the goal, such as tremendous throughput gain in the study of [11], is recommended.

In general, two kinds of conventional CRN scenarios are usually considered. The first one is that CRN is a collection of CR nodes executing the same set of networking protocols (as the scenario in IEEE 802.22 [12]–[15]), as shown in Fig. 1(a). In this case, all links are opportunistic links established by CR nodes using the secondary system protocol. Thus, the most critical characteristic is that the transmissions within CRN should be well coordinated without interference causing outage to PS. In [14], it has been shown that network throughput improvement of the overall CRN through the network-coding techniques can be achieved. The other conventional CRN scenario is a collection of heterogeneous wireless networks in which the CR nodes facilitate the coexistence and efficient exploitation of heterogeneous networks (as the scenario in IEEE P1900.4 and ETSI RRS [16]–[19]), as shown in Fig. 1(b). Through the cognitive capability, CRN could overcome the problems in conventional networks, such as the unawareness of network status and the lack of intelligent adaptation, by observing, reacting, learning, and adapting to various environment stimuli [20]. On the other hand, extending from the preceding conventional CRN scenarios, we can further define the general-sense CRN scenario as a collection of CR nodes and nodes of coexisting multiradio systems, including PSs exciting the same set of CR networking protocols on top of existing networking (as in [11] and [21]), as shown in Fig. 1(c). The links might adopt PS protocols or secondary system protocols. That is, the nodes of all coexisting multiradio systems, including both PSs and secondary systems, can cooperatively be interconnected and internetworked. Within such a CRN, the packets from a source node would reach a destination node through multihop/multipath cooperative relay networks composed of PS network(s) and/or secondary system network(s). It is shown in [11] that, through randomly generated topology simulation, the overall network

Manuscript received February 10, 2010. First published March 8, 2010; current version published May 14, 2010. This work was supported by the National Science Council of Taiwan under Contract NSC 98-2219-E-002-018. The material in this paper was presented in part at the Spring IEEE Vehicular Technology Conference, May 2008, and at the Spring IEEE Vehicular Technology Conference, April 2009. The review of this paper was coordinated by Dr. W. Zhuang.

The authors are with the National Taiwan University, Taipei 106, Taiwan (e-mail: r95942061@ntu.edu.tw; chenkc@cc.ee.ntu.edu.tw; smcheng@cc.ee.ntu.edu.tw).

Color versions of one or more of the figures in this paper are available online at http://ieeexplore.ieee.org.

Digital Object Identifier 10.1109/TVT.2010.2044906

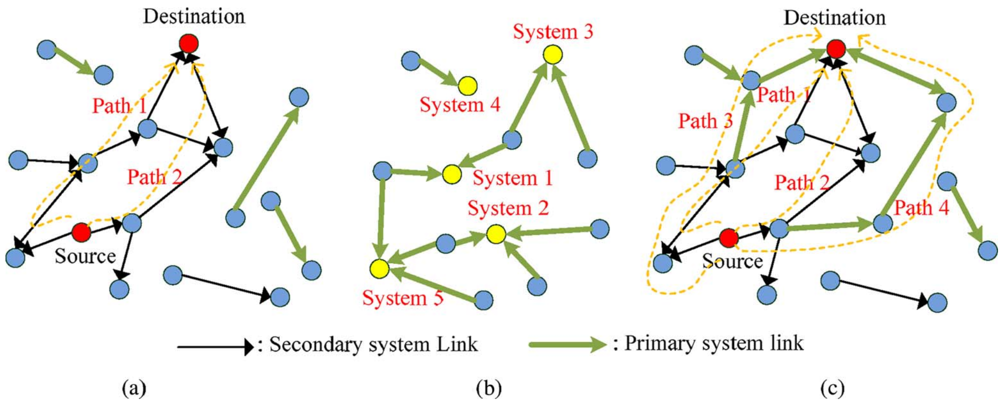

Fig. 1. (a) Conventional CRN-1: Collection of CR nodes with the routing task accomplished by the secondary system links to connect CR nodes. (b) Conventional CRN-2: Collection of heterogeneous wireless networks where the CR nodes facilitate the coexistence and efficient exploitation of heterogeneous networks. (c) General-sense CRN: Collection of CR nodes and nodes of coexisting multiradio systems including PSs with the routing task accomplished by secondary system links or PS links to cooperative relay packets.

capacity of the general-sense CRNs through network coding study can significantly be enhanced and compared. On the other hand, by grouping multiple relay paths, the statistical quality-of-service guarantees are provided in [22] and [23]. These results promote us to leverage PS or coexisting wireless networks to cooperatively relay packets. Throughout this paper, we consider the general-sense CRN scenario as the complete networking scenario for the terminology "cognitive radio network."

B. General Sensing Capability of CRN: CRN Tomography

In conventional CR link (opportunistic) communication between a transmitter–receiver pair, the key enabling functionality of CR would be spectrum sensing facilitated by detection and estimation to supply the information to determine whether the spectrum "hole" for the secondary system link is available. Spectrum sensing here is defined to monitor the spectrum bands, to capture information bearing in spectrum bands, and then to detect the spectrum holes according to the received signal [24]. Another CR sensing case would be location awareness to obtain the accurate location information [25]–[30]. A cognitive positioning system that achieves accuracy in both indoor and outdoor environments is proposed with adaptive time of arrival [28], and the fundamental limits on time delay estimation for CR positioning are further studied in [30].

However, when we consider the CRN scenario, the requirement of more information toward networking the CR nodes and PS nodes beyond link establishment induces the need for a more general and powerful sensing methodology of CRN. For example, CR nodes have to sense the active coexisting/neighboring communication systems for the potential cooperation. Another obvious example may be the routing function of CRN where CR nodes have to determine whether the neighboring nodes (either CR nodes or PS nodes) are reliable and trustworthy for cooperative packet relay. To reliably capture information for multilink operations and networking functions in CRN, methodologies beyond link-level sensing are necessary to generalize CR spectrum sensing based on detection and estimation.

A well-known methodology to acquire network-level knowledge is the cognitive pilot channel (CPC) [31], [32] in ETSI RRS [33] or a similar concept, i.e., Radio Enabler, in IEEE P1900.4 [17], [18], [34]. The CPC uses an invariable radio link to convey, in real time, all necessary information to CR nodes concerning the available frequency bands, radio access technology, services, load situation, network policies, etc., so that terminals can be reconfigured to connect to whatever service that is available on whatever frequency [16]. According to the information brought by CPC, the corresponding network-selection strategy is developed in [35] and [36]. Since CR nodes might avoid a scanning process of spectrum and networks, they would benefit from lower battery consumption and connection setup time. However, CPC requires additional constructing cost such as common control channel bandwidth and thus is not always available when we consider a general environment such as the coexistence of multiple systems and standards. In this case, a kind of methodology via statistical inference and learning, which is generalized and extended from CR link-level spectrum sensing and without assuming any available control/signaling channel to acquire information such as CPC performed in ETSI RRS and radio enabler defined in IEEE P1900.4, is necessary and should be developed. This new framework of technology is named *CRN tomography*, borrowing the terminology from well-known medical imaging and network tomography by Vardi [37].

Definition 1.1 (CRN Tomography): CRN tomography is a sort of statistically measuring, processing, and inferring techniques that provide the parameters and traffic/interference patterns for CRN operations at both the link and network levels.

Conventional CR spectrum sensing to detect spectrum hole and location awareness to discover the distances among CR nodes fall into straightforward scenarios of CRN tomography. However, CRN tomography is a general term to embrace such techniques without assuming any available control/signaling channel to acquire information. According to the CRN tomography concept, we can then establish a novel framework of CRN tomography, which can be helpful for systematical explorations of appropriate inference techniques for CRN operations. CRN tomography shall generally consist of the acquisition of the required information for conventional CR link transmissions (and, thus, OSA) and CRN network operations (and, thus, to leverage available network resources). Due to the extremely limited radio resource among the coexisting multiradio primary/secondary systems and the nature of stochastic radio links [38], [39], the information inferring of CRN tomography is beyond the scope of Internet tomography [40]. Generally speaking, there are three main challenges in CRN tomography: 1) to acquire information without extra cooperation among heterogeneous networks; 2) to infer the parameter without real-time (or online) feedback information in asymmetric or unidirectional links; and 3) to acquire the information of multilink operations under the dynamic environments. Together with these challenges, CRN tomography can supply much information beyond conventional network inference and existing spectrum-sensing techniques.

The first challenge arises from the fact that CRN would generally be composed of heterogeneous coexisting multiradio networks. Unlike typical wireless infrastructure or ad hoc networks, CRN can operate as a deregulated or unlicensed, massive, and even complex network [41] due to the coexistence and interaction of multiple heterogeneous radio networks. Nodes in CRN may operate multiple wireless communication technologies, protocols, backbone network types, user terminal types, network operators, etc. The nodes within a CRN may lack full connection and cooperation, even within the radio range or even if they execute an identical wireless protocol, due to trust and security network functioning [21] or no cooperation responsibility (for PS) with other coexisting systems. It creates new challenges to acquire desirable information.

The second challenge arises from the property that the links of CRN are generally opportunistic, asymmetric, or unidirectional [38], [39], [42], which creates challenges to feedback real-time and perfect information from the destination to the source (e.g., ACK). The opportunistic and unidirectional link is a special nature of CRN. Considering a link between CR node A and CR node B in CRN, node A having an opportunity to transmit to node B in a certain time duration does not warrant an opportunity for node B to transmit to node A. The security and/or traffic control of intersystem operations suggests another possible unidirectional scenario. When CR nodes leverage an existing PS networks to relay packets, the successful transmission from a CR node to PS network does not necessarily warrant the permission of transmission in the reverse direction. Therefore, in addition to imperfect real-time observations through detection and estimation techniques, CRN tomography should further utilize information derived from statistical inference based on the available (delayed) observations.

Finally, CRN network layer functions, such as routing and flow control, might need information about multiple neighboring nodes with multiple hops in depth. The multilink operations are resulted from multiradio links from one node and multihop connections between two nodes. The communication environment of CRN is quite dynamic due to OSA and channel variations and introduces challenges to reliably acquire information related to multilink operations. On the other hand, since the opportunistic links induce the rapid variations of CRN topology, the information across multihop connections suffers from delay or limited bandwidth or even unavailability due to unidirectional links. Therefore, CRN tomography has to robustly acquire appropriate and precise information for multilink operations under highly dynamic environments.

TABLE I
FRAMEWORK OF CRN TOMOGRAPHY

Tomography Operation	Link-Level Parameter	Network-Level Parameter
Passive Monitoring	Section III-A (e.g. Spectrum Hole Detection)	Section III-B (e.g. Multiple-System Sensing)
Active Probing	Section IV-A (e.g. Radio Resource Sensing)	Section IV-B (e.g. Success Probability Estimation)

We particularly note that many techniques exist for specific parameters in CRN. Nevertheless, they belong to part of an overall CRN tomography framework as special cases. What we intend to provide in this paper is a novel framework of CRN tomography, which can be helpful for systematical explorations of appropriate inference techniques for CRN operations. In this paper, we target at CRN environment and operations well beyond just detection of spectrum holes or white space, which is a novel scenario beyond traditional communication networks and inherently with new challenges.

C. Contribution and Summary

In this paper, we propose CRN tomography as the generalized spectrum sensing of a CRN node, including traditional sensing based on detection and estimation at the link level and inferring at the link and multilink (i.e., network) levels. We first establish the framework of CRN tomography to provide systematic approaches to develop and to classify appropriate CRN tomography techniques. Specifically, CRN tomography provides a methodology to deliver information for spectrum management and network activities in the heterogeneous and decentralized CRN via statistical inference or learning algorithms. The framework of CRN tomography is developed via two aspects, i.e., *tomography operation* and *tomography parameter* as Table I.

1) *Tomography operation*: Based on the tomography operation, techniques for CRN tomography can be classified into passive monitoring or active probing. Most traditional spectrum-sensing techniques belong to passive monitoring for the detection of the transmitter signals [43]–[64]. However, active probing under controllable interference for network operation can infer more network information, e.g., a cognitive positioning system of location awareness techniques [28] and request-to-send/clear-to-send in IEEE 802.11 wireless LANs [65]. Since there is rarely a study regarding active probing in CRN, we systematically present the active probing for both link- and network-level inferences in CRN information collection in Section IV, which shows the possibly great improvement of active probing in CRN.
2) *Tomography parameter*: Another general purpose of spectrum sensing is to acquire information about system/network parameters. CRN takes care of not only link-level transmission (transmitter–receiver) among nodes but network-level operations (source–destination) routing over multiple links [66], beyond conventional CR research, as well. Generally speaking, the target parameters

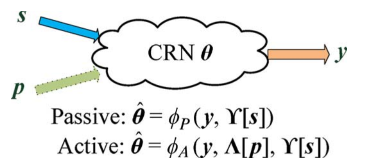

Fig. 2. Schema of CRN tomography.

of CRN tomography are at either the link or the network level. Section III (passive monitoring) and Section IV (active probing) present techniques to obtain tomography parameters at both the link and network levels.

Consequently, we have four categories for CRN tomography techniques: 1) passive link-level monitoring; 2) passive network-level monitoring; 3) active link-level probing; and 4) active network-level probing.

II. Classifications of Cognitive Radio Network Tomography Techniques

A. Passive Monitoring and Active Probing

Generally speaking, active probing of CRN tomography involves explicit transmission of a probing signal or implicitly derives information from traffic. Passive monitoring to avoid potential interference plays a dominating role in current spectrum-sensing research, whereas active probing is introduced to require or to infer information through the transmission of probing signal, under the controlled interference. As Fig. 2, the message flow $\boldsymbol{s}$ originally exists in CRN, $\boldsymbol{\theta}$ is the unknown information of interests, and $\boldsymbol{y}$ represents observations taking values in an observation set $\boldsymbol{\Gamma}$, which may be a set of vectors, waveforms, events, or any other set, with random nature. The purpose of CRN tomography is to infer (or to detect or to estimate) $\boldsymbol{\theta}$ according to $\boldsymbol{y}$ and full/partial information about s, where we use an information extraction function $\Upsilon[\boldsymbol{s}]$ to characterize *a priori* knowledge of $\boldsymbol{s}$.

For passive monitoring, we can obtain the inference result of $\boldsymbol{\theta}$ and $\hat{\boldsymbol{\theta}}$ by

$$\hat{\boldsymbol{\theta}} = \phi_P\left(\boldsymbol{y}, \Upsilon[\boldsymbol{s}]\right) \tag{1}$$

where $\phi_P(\cdot,\cdot)$ is the passive inferring rule. Taking the observations $\boldsymbol{y}$, kinds of techniques can be developed. Passive monitoring is widely considered as spectrum sensing in CR by inferring the target information without interfering the traffic and behavior of CRN. Nevertheless, they can merely be applied when observations are sufficient for provision of the inference of $\boldsymbol{\theta}$. Sometimes, the available observations are not (or insufficiently) related to the target information, which invokes difficulties to reliably infer $\boldsymbol{\theta}$ for passive monitoring, such as the hidden terminal problem of spectrum/carrier sensing in [53].

Departing from traditional thinking, active probing may provide an alternative to obtain additional critical information beyond passive monitoring, which will be discussed in Section IV. Generally speaking, in active probing, the probing signal is transmitted to induce or enhance the correlation between the target information and observations (and thus provide extra knowledge for inference) surely under controllable interference. The probing signal $\boldsymbol{p}$ may be completely or partially known beforehand, and we use the information extraction function $\Lambda[\boldsymbol{p}]$ to characterize *a priori* knowledge of $\boldsymbol{p}$. Hence, $\hat{\boldsymbol{\theta}}$ is determined in active probing by

$$\hat{\boldsymbol{\theta}} = \phi_A\left(\boldsymbol{y}, \Lambda[\boldsymbol{p}], \Upsilon[\boldsymbol{s}]\right) \tag{2}$$

where $\phi_A(\cdot,\cdot,\cdot)$ is the active inferring rule. When active probing is used, it should be noted that the probing signal must not significantly distort the network or link traffic or behavior of CRN.

Equations (1) and (2) are general expressions to describe the progress of information inference for passive and active CRN tomography, respectively. We present them here to systematically and scientifically represent the concept of CRN tomography for the CRN tomography framework.

B. Link- and Network-Level Parameter

The target tomography parameter is another way to classify the techniques of CRN tomography. In general, the link-level parameters are referred to the parameters for the establishment of links between a transmitter node and a receiver/listening node, such as those for spectrum sensing, spectrum access, and distance awareness among nodes. Although there already exists a vast amount of research at the link level, the statistical inference (rather than detection/estimation) of link-level parameters still plays a novel role in CRN operations, owing to the opportunistic links of CRN. On the other hand, the network-level parameters take the responsibility of network layer functions in multiple links, as considered in two aspects in Section I-B, such as network access, packet routing, and mobility management. The parameters for the multilink network level are seldom addressed in conventional CR study; however, they are essential for CRN scenarios, particularly multilink operations and cooperative networking.

Throughout this paper, we assume that, in CRN, PS links (primary links) and secondary system links (cognitive links) are logically numbered and form sets $\mathbf{L}_P = \{1, \ldots, L_P\}$ and $\mathbf{L}_C = \{1, \ldots, L_C\}$, respectively, and there is a set of numbered nodes $\mathbf{V} = \{1, \ldots, V\}$. In link-level exploration, we consider the operation of a specific cognitive link $l_C \in \mathbf{L}_C$. The overall spectrum is separated as a set of numbered channels $\mathbf{M} = \{1, \ldots, M\}$, where the mth channel is with frequency bandwidth B_m. We suppose that, for the mth channel, the CR transmitter (CR-Tx) and the CR receiver (CR-Rx) are synchronously operating with the sensing period T_m and the sensing interval t_m^s to periodically sense the spectrum. The rest of time $t_m^a = T_m - t_m^s$, which is known as the allocation interval, is used to transmit signals in accordance with the sensing and allocation results. A special case for the synchronous communication of primary and cognitive links is that the sensing period T_m and the sensing interval t_m^s are equal for all channels.

III. Passive Monitoring

We start by briefly reviewing and characterizing conventional spectrum sensing, including numerous well-known techniques in the CR technique.

A. Link-Level Parameter Inference

The most well-studied and well-known passive link-level monitoring of CRN tomography is spectrum sensing. In general, spectrum sensing is to passively detect the spectrum holes among CR nodes under the PS operating and coexisting environment. Consider the spectrum-sensing techniques developed under the interweave spectrum-sharing approach, in which the temporary frequency band voids are referred to as the spectrum hole, meaning that no PS is active in this frequency band at this timing. When a specific PS operates in the mth channel, spectrum sensing is to decide between two hypotheses

$$y[n] = \begin{cases} w[n], & H_0 \\ as[n] + w[n], & H_1 \end{cases}, \qquad n = 1, \ldots, N \tag{3}$$

within the sensing interval t^s_m, where $y[n]$ is the complex signal received by the CR-Rx, $s[n]$ is the transmitted signal of the primary transmitter (PS-Tx), $w[n]$ is the additive white Gaussian noise (AWGN), and a is the complex gain of an ideal channel. H_0 represents the hypothesis that no primary signal is present, and thus, the spectrum hole is detected. H_1 represents the hypothesis that a primary signal exists, and thus, no spectrum hole is detected. For example, when we consider the IEEE 802.22 environment to detect the TV broadcasting signal, referring to (3), $s[n]$ represents the TV signal, and H_0 means that the spectrum hole is detected. Note that the system model in (3) can also be applied to orthogonal frequency-division multiplexing (OFDM) PSs where each channel represents a specific subcarrier to determine whether this subcarrier is unused and to CDMA PSs, where each channel represents a specific code. We can reformulate the spectrum hole detection problem in the framework of CRN tomography:

Proposition 3.1 (Spectrum Hole Detection): We can rewrite (3) as

$$\boldsymbol{y} = \mathbb{I}^P_{\text{active}} \cdot a\boldsymbol{s} + \boldsymbol{w} \tag{4}$$

where $\boldsymbol{y} = [y[1], \ldots, y[N]]^T$ is the observation vector, $\boldsymbol{s} = [s[1], \ldots, s[N]]^T$ is the message flow vector, $\boldsymbol{w} = [w[1], \ldots, w[N]]^T$ is the noise vector, and $\mathbb{I}^P_{\text{active}}$ is an indicator function that is equal to 1 if the PS-Tx is transmitting and equal to 0 otherwise. This detection problem can be reformulated as the CRN tomography problem, where the target vector $\boldsymbol{\theta}$ is the indicator $\mathbb{I}^P_{\text{active}}$ function in this case.

According to *a priori* information about $\boldsymbol{s}$, many famous spectrum-sensing techniques including an energy detector, matched filter, cyclostationary detection, and wavelet detection are developed to infer $\mathbb{I}^P_{\text{active}}$ using passive monitoring due to the fact that CR-Rx passively listens to the radio signals from PS-Tx. When the observations of multiple CR-Rx are available, cooperative spectrum sensing would be helpful for better detection performance as it exploits sensor diversity via simultaneous sensing on a channel at multiple locations. The existing spectrum-sensing techniques are summarized in Table II, whereas the feasibility of the spectrum-sensing techniques is addressed and experimented in [64].

Remarks: The passive link-level monitoring can be applied beyond the spectrum-hole-detection problem. For example, to optimize the MAC-layer sensing and efficiently discover spectrum opportunities, the cognitive link availability as a probability measure is critical. In [67], the maximum likelihood (ML) and confidence interval of estimators are adopted to estimate the underlying channel-usage patterns as passive link-level monitoring.

TABLE II
SUMMARY OF CONVENTIONAL CR SPECTRUM-SENSING TECHNIQUES

Spectrum Sensing Algorithm	Description	Reference
Energy detection	Estimate the energy in a frequency band and compare against a detection threshold.	[43]–[46]
Cyclostationary detection	Compute the spectral correlation function and detect the peak at multiples of the modulation rate/frequency.	[47]–[51]
Matched Filter	Coherently detect the pilot signals.	[52]–[54]
Wavelet detection	Employ a wavelet transform of PSD of the observed signal to locate the singularities of the PSD and identify the vacant frequency bands.	[55]–[57]
Cooperative Detection	Fuse the observation signal to the fusion center/other nodes and combine them to make decision.	[58]–[63]

B. Network-Level Parameter Inference

After successfully presenting conventional CR spectrum sensing as the passive link-level monitoring in CRN tomography, we further generalize the passive tomography to infer parameters for multilink network operation. An immediate challenge regarding CRN comes from the identification of system parameters among coexisting multiradio systems/networks (such as scenario for IEEE 802.19). This is known as *multiple-system sensing*, in which CR-Rx senses and identifies the coexisting active communication systems for possible cooperative packets relay, such as systems at a 2.4-GHz industrial, scientific, and medical (ISM) band.

To conduct cooperative relay over coexisting multiradio (heterogeneous) systems/networks, CR nodes have to quickly associate to a selected node of CRN (either a PS or a CR node) in a very short available time duration due to the dynamic and opportunistic CRN environment [38], [66]. Consequently, the multiple-system sensing (or identification) is essential at the initial stage of association (to a selected system) for CR nodes. The critical challenge for the multiple-system sensing problem is the intersystem interference. Conventional techniques used in spectrum sensing may work when only one specific PS is possible in the target spectrum. However, when multiple systems coexist in the spectrum, i.e., the signals might be overlapped in the spectrum, the intersystem interference dominates spectrum-sensing techniques. For example, the energy detection technique can only distinguish the existence of any active system(s). Therefore, a more reliable and general algorithm is needed for multiple coexisting systems by applying three techniques together to accomplish the multiple-system sensing: 1) fundamental frequency; 2) power spectrum density pattern; and 3) fourth-order cumulant.

1) System Model: Assume that there are Q candidate communication systems with known system parameters, and each system has one transmitter. The transmitted signal of each system goes through a flat uncorrelated Rayleigh-fading channel with an independent complex channel amplitude $a_i = |a_i| \cdot e^{j\theta_i}$, where amplitude $|a_i|$ is Rayleigh distributed with $E|a_i|^2 = \gamma_i^2$ and phase θ_i is uniformly distributed over $[0, 2\pi]$. In addition, a white Gaussian noise $w(t)$ with zero mean and variance σ_w^2 is added to the received radio signal. Suppose that the activities of the systems remain unchanged during the sensing interval. With the assumption of K active systems ($K \leq Q$), the radio signal received by CR-Rx can be expressed as

$$y(t) = \mathrm{Re}\left\{\sum_{i=1}^{K} a_i s_i(t) + w(t)\right\} = \mathrm{Re}\left\{c(t) + w(t)\right\} \quad (5)$$

where $s_i(t)$ is the signal of the ith active system, and $c(t) = \sum_{i=1}^{K} a_i s_i(t)$. Note that the system model can be applied to the transmitted signals of multiple systems within the same frequency band, and we do not specify what kinds of signals $s_i(t)$ they are, e.g., OFDM, directed-sequence spread spectrum, and frequency-shift keying signals.

Proposition 3.2 (Multiple-System Sensing): The radio signal received by CR-Rx can be rewritten in discrete time as

$$\boldsymbol{y} = \sum_{i=1}^{Q} \mathbb{I}_{\text{active}}^{P}[i] \cdot a_i \boldsymbol{s}_i + \boldsymbol{w} \quad (6)$$

where $\boldsymbol{y} = [y[1], \ldots, y[N]]^T$ is the observed signal vector, a_i is the complex channel gain from the transmitter of the ith system to the CR node, $\boldsymbol{s}_i = [s_i[1], \ldots, s_i[N]]^T$ is the transmitted signal vector of the ith system, $\boldsymbol{w} = [w[1], \ldots, w[N]]^T$ is the noise vector, and $\mathbb{I}_{\text{active}}^{P}[i]$ is the indicator function that is equal to 1 if the transmission of the ith system is active and equal to 0 otherwise. The target parameter $\boldsymbol{\theta}$ is the indicator vector $\mathfrak{I}_{\text{active}}^{P} = [\mathbb{I}_{\text{active}}^{P}[1], \ldots, \mathbb{I}_{\text{active}}^{P}[Q]]^T$.

According to *a priori* information, different unique characteristics of candidate systems can be exploited. In the following, we propose an algorithm to infer $\mathfrak{I}_{\text{active}}^{P}$ by three methods, i.e., fundamental frequency, power spectrum density pattern, and fourth-order cumulant, where the detail of the derivation can be referred to [68].

2) Fundamental Frequency: Typical signaling in digital communication systems gives energy peak(s) in the reciprocal of the symbol period (baud rate) and in its harmonics. The fundamental frequency is defined as the lowest frequency (baud rate). Suppose that these P active systems are digital communication systems with fundamental frequency characteristic. The transmitted signal of the ith system may be written in the form

$$s_i(t) = \sum_{n=-\infty}^{\infty} x_{i,n} h_i(t - nT_i - \tau_i) e^{j(2\pi f_{c,i} t + \alpha_i)} \quad (7)$$

for $i = 1, 2, \ldots, K$, where $\{x_{i,n}\}$ is the data sequence; $h_i(t)$ is the impulse response of the pulse-shaping filter with frequency response $H_i(j\omega)$; T_i is the symbol duration; $\tau_i \in [0, T_i)$ and $\alpha_i \in [0, 2\pi)$ are the time offset and the phase offset, respectively (with both being regarded as constants during sensing); and $f_{c,i}$ is the carrier frequency. We specifically assume that $\{x_{i,n}\}$ is zero mean variance σ_i^2 stationary sequences with statistically independent and identically distributed elements.

There are various methods to extract the fundamental frequency information [47], and here, we adopt the nonlinear spectral line method with squared magnitude, followed by a narrowband bandpass filter. Assuming $c(t)$ with equal variance in real and imaginary parts and independent of $w(t)$, which is a regular condition in a conventional digital system, $E\{y^2(t)\} = 1/2 \cdot E\{|c(t)|^2 + |w(t)|^2\}$. The squared signal $y^2(t)$ can be decomposed as $E\{y^2(t)\}$ and $\varepsilon(t)$, where $\varepsilon(t)$ is a disturbance term with zero mean, and thus becomes

$$y^2(t) = \frac{1}{2}\sum_{i=1}^{K} \frac{\sigma_i^2 \gamma_i^2}{T_i} Z_{i,1} \cos\left[\frac{2\pi(t-\tau_i)}{T_i}\right] + \frac{1}{2}\sum_{i=1}^{K} \frac{\sigma_i^2 \gamma_i^2 Z_{i,0}}{T_i} + \frac{1}{2}\sigma_w^2 + \varepsilon(t) \quad (8)$$

where $Z_{i,m} = (1/2\pi)\int_{-\infty}^{\infty} H_i(j\theta) \cdot H_i^*(-j((2\pi m/T_i) - \theta)) d\theta$. We can observe spectral line terms at frequencies $\{1/T_i\}$ in (8). After filtering the signal with a narrowband bandpass filter containing all potential fundamental frequencies, these tones can easily be detected to identify the corresponding systems. The derivation detail of (8) is skipped and can be referred in [68].

3) Power Spectrum Density Pattern: The transmitted signals from the active systems could be coupled in the received radio signal of CR-Rx. Thus, the received power spectrum density is contributed by all active systems' signals. Under the reasonable assumption that the power spectrum density patterns of all candidate systems are known *a priori* and linear independent, we can identify the active systems by performing well-known singular value decomposition (SVD) to resolve the linear combination of the received power spectrum density.

Suppose that the power spectrum density of each candidate system is known and portioned into Z equal-bandwidth subbands. The received signal in discrete time can be written as $y[n] = \sum_{i=1}^{K} a_i s_i[n] + w[n]$, where $s_i[n]$ is the transmitted signal of the ith candidate system in discrete time with unknown power σ_i^2 and known power spectrum density pattern $\mathbf{p}_i \equiv [P_i(1), P_i(e^{j2\pi/Z}), \ldots, P_i(e^{j2\pi(Z-1)/Z})]^T$. Assume that these power spectrum density patterns $\{\mathbf{p}_i\}_{i=1}^{Q}$ are linear independent. After spectrum estimation (assuming enough observation length is available and thus the power spectrum estimation error can be neglected), the resulting signal can be expressed in vector form as $\hat{\mathbf{p}} = \sum_{i=1}^{K} \gamma_i^2 \sigma_i^2 \mathbf{p}_i + \mathbf{w} = \mathbf{S} \cdot \mathbf{h} + \mathbf{w}$, where $\hat{\mathbf{p}} \equiv [\hat{P}(1), \hat{P}(e^{j2\pi/Z}), \ldots, \hat{P}(e^{j2\pi(Z-1)/Z})]^T$ and $\hat{P}(e^{j2\pi z/Z})$ is the estimation at frequency $\omega_z = 2\pi z/Z$, $\mathbf{S} \equiv [\mathbf{p}_1, \mathbf{p}_2, \ldots, \mathbf{p}_Q]_{Z \times Q}$ is the power spectrum pattern matrix, $\mathbf{w} \equiv [W(1), W(2), \ldots, W(M-1)]^T$ is the noise power spectrum, and $\mathbf{h} \equiv [\gamma_1^2\sigma_1^2, \gamma_2^2\sigma_2^2, \ldots, \gamma_Q^2\sigma_Q^2]^T$ is ideally with K nonzero elements. Note that we assume that the noise power spectrum is slow varying and can accurately be estimated.

Since $\{\mathbf{p}_i\}_{i=1}^{Q}$ are linear independent, $\mathbf{S}$ is a $Z \times Q$ matrix of rank Q. By performing SVD, $\mathbf{S}$ can be decomposed as

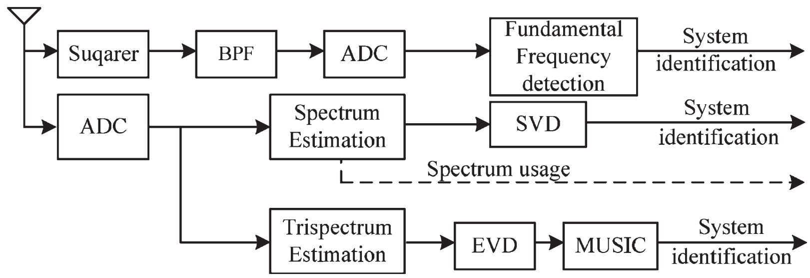

Fig. 3. Block diagram of the general multiple-system sensing algorithm.

$\mathbf{S} = \mathbf{U}\mathbf{\Lambda}\mathbf{V}^T$, where $\mathbf{U}$ and $\mathbf{V}$ are a $Z \times Z$ orthogonal matrix and a $Q \times Q$ orthogonal matrix, respectively, and $\mathbf{\Lambda}$ is a $Z \times Q$ matrix with (i, j)-entry $s_{ii} = \varsigma_i$ for $i = 1, 2, \ldots, Q$ and $s_{ij} = 0$ otherwise, where $\{\varsigma_i\}_{i=1}^{Q}$ are the singular values of $\mathbf{S}$. Therefore, we can solve $\mathbf{h}$ by

$$\mathbf{V}\mathbf{\Lambda}^+\mathbf{U}^T(\hat{\mathbf{U}} - \mathbf{w}) = \mathbf{V}\mathbf{\Lambda}^+\mathbf{U}^T\mathbf{U}\mathbf{\Lambda}\mathbf{V}^T\mathbf{h} = \mathbf{h} \qquad (9)$$

where $\mathbf{\Lambda}^+$ is a $Q \times Z$ matrix with (i, j)-entry $q_{ii} = 1/\varsigma_i$ for $i = 1, 2, \ldots, Q$ and $q_{ij} = 0$ otherwise.

Ideally, $\mathbf{h}$ contains nonzero elements only when the corresponding systems are active. In practice, $\mathbf{h}$ is always nonzero because of estimation errors. A serial search can be applied by arranging the elements of $\mathbf{h}$ in decreasing order, i.e., $k_1 \geq k_2 \geq \cdots \geq k_Q$. Compute the ratio $\sum_{i=1}^{\hat{K}} k_i / \sum_{i=1}^{Q} k_i$ from $\hat{K} = 1$, and stop when the ratio exceeds a predetermined threshold. When the search stops, the number of active systems is determined as $\hat{K}$, and the corresponding elements and systems are identified.

4) Fourth-Order Cumulant: We explore the characteristic of power spectrum density pattern based on the additive Gaussian noise with known covariance matrix. However, if the covariance matrix of the additive noise is unknown, the resulting signal, which is a linear combination of spectrum vectors, cannot uniquely be solved. This implies that only the power spectrum density pattern (belonging to the second-order statistics) is not sufficient to detect and identify the systems. High-order statistics in which cumulants are blind to any kind of Gaussian process [69] becomes useful to ensure the success of the multiple-system sensing, whereas a similar problem is investigated in [70] to detect and classify multiple sources by a single sensor.

Suppose that the transmitted signal $s_i[n]$ is modeled as a non-Gaussian random process with fourth-order cumulant ρ_i convolving a spectrum-shaping filter $h_i[n]$ with a frequency response $H_i(e^{j\omega})$ that $|H_i(e^{j2\pi z/Z})|^2 \equiv P_i(e^{j2\pi z/Z})$ for $z = 0, \ldots, Z-1$, where the power spectrum density pattern $\mathbf{p}_i$ is known and $\{\mathbf{p}_i\}_{i=1}^{Q}$ are linear independent. The $Z \times Z$ trispectrum matrix $\mathbf{C}$ can be expressed as

$$\mathbf{C} = \sum_{i=1}^{K} \gamma_1^4 \rho_i \mathbf{p}_i \mathbf{p}_i^T = \mathbf{S}\mathbf{\Gamma}\mathbf{S}^T \qquad (10)$$

and $\mathbf{\Gamma}$ is a $Q \times Q$ diagonal matrix with only K nonzero diagonal elements. Ideally, $\mathbf{C}$ is a real symmetric matrix with rank K, and the number of active systems can be determined by computing the rank of $\mathbf{C}$. Unfortunately, in practice, the estimation of $\mathbf{C}$ is always of full rank because of estimation error. By performing an eigendecomposition on the estimation of the trispectrum matrix, $\hat{\mathbf{C}}$ can be written as

$$\hat{\mathbf{C}} = \sum_{z=1}^{Z} \lambda_z \mathbf{g}_z \mathbf{g}_z^H = \mathbf{G}\mathbf{\Sigma}\mathbf{G}^H \qquad (11)$$

with the eigenvalues arranged in decreasing order. The signal subspace is spanned by $\{\mathbf{g}_i\}_{i=1}^{K}$, and the noise subspace is spanned by $\{\mathbf{g}_i\}_{i=K+1}^{Z}$. Therefore, the number of active systems and system identification can proceed by serial search and the MUSIC algorithm, respectively. Compute the MUSIC pseudospectrum

$$\overline{R_{\text{music}}}(i) = \frac{\mathbf{p}_i^H \mathbf{p}_i}{\sum_{z=K+1}^{Z} |\mathbf{p}_i^H \mathbf{g}_z|^2} \qquad (12)$$

and the systems with the corresponding K largest values are selected and identified as active ones. Ideally, the trispectrum matrix in (10) is not affected by the power of additive Gaussian noise σ_w^2, which means that the fourth-order cumulant methodology is expected to perform well in low-signal-to-noise-ratio environment.

5) General Multiple-Sensing Algorithm: As a summary, we propose the general multiple-system sensing that exploits the preceding three system-specific characteristics to identify the spectrum utilization status and the active system(s) over uncorrelated Rayleigh-fading channels. The block diagram of the general multiple-system sensing algorithm is shown in Fig. 3.

Algorithm 1 General Multiple-System Sensing Algorithm
1: Energy detection and carrier locking to initiate the algorithm.
2: Square the received radio signal and filter it by a narrowband bandpass filter containing all potential fundamental frequency. Detect the fundamental frequencies, and identify the corresponding systems (Section III-B2).
3: Estimate the power spectrum density of the target spectrum.
4: If the result of step 2 is none, end; otherwise, go to step 5.
5: If the covariance matrix of noise is known, go to step 6; otherwise, go to step 7.
6: Perform SVD of the spectrum estimation result, and identify systems (Section III-B3). End.
7: Estimate the trispectrum matrix of the target spectrum. Perform eigenvalue decomposition of the trispectrum matrix, and identify systems by MUSIC algorithm (Section III-B4). End.

TABLE III
SYSTEM PARAMETERS

System	Carrier Frequency	Fundamental Frequency
802.11b	2412, 2437, 2462 MHz	11 MHz
802.11g	2412, 2437, 2462 MHz	20 MHz
Bluetooth	Not fixed	1 MHz
Microwave Oven	None	None

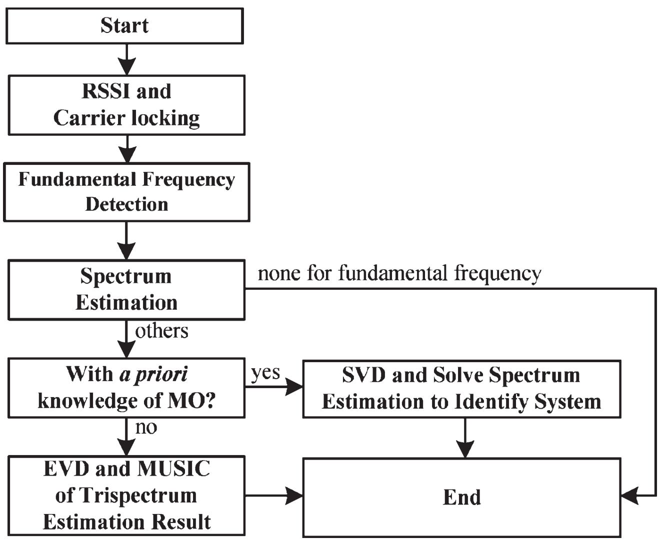

Fig. 4. Flowchart of multiple-system sensing for the 2.4-GHz-band example.

6) Example—Multiple Coexisting Systems at 2.4-GHz ISM Band: We consider multiple coexisting systems at the 2.4-GHz ISM band, which includes a wireless local area network (802.11b and 11g), Bluetooth, and the microwave oven as potential active systems. The system parameters for the ordinary operating environment are listed in Table III. The flowchart of multiple-system sensing for this example is shown in Fig. 4. When energy detection indicates the potential existence of active systems in the spectrum, we try to lock the carrier frequency to 2412, 2437, and 2462 MHz. If some carrier frequencies are locked, it implies that 802.11b or/and 802.11g systems exist in the corresponding channels. If none is locked, there is no active 802.11b or 802.11g system. We next apply the fundamental frequency method. Since squaring a very broadband radio-frequency spectrum might be difficult, the entire frequency band could be divided into several subbands to proceed the sensing task. The fundamental frequency method can help to determine the existence of 802.11b, 802.11g, and Bluetooth systems from their different fundamental frequencies. After spectrum estimation, we can obtain the status of spectrum usage. If we know the power spectrum density of the microwave oven, the power spectrum density pattern method can be exploited. If the power spectrum density of the microwave oven is unknown, but the microwave oven interference is modeled as an additive Gaussian noise, the fourth-order cumulant method can be applied to identify the existence of other active systems with non-Gaussian signals.

Remarks: In this section, we attempt to address the challenges in multiple-system sensing problems, particularly for CRN, and to demonstrate that the multiple-system sensing can be dealt with by the combination of existing methods, which belong to passive network-level CRN tomography. Passive monitoring for network-level parameter(s) may be suitable when the overhead of network connection and transmission is rare or unavailable. For example, in multiple-system sensing, the attempted connection to each candidate system would require optimal identification performance since it has a short time window under the dynamic and opportunistic link availability in CRN.

IV. ACTIVE PROBING

Up to this point, we have emphasized the representation of passive monitoring, which is often convenient and useful to serve the purpose of CR link establishment. However, an innovative thinking is to introduce a probing signal into the CRN, surely under controlled interference to CRN operation, to obtain information and/or parameter(s) for CRN network-level operation by inference from the response of the probing signal. Since the idea is just like medical tomography or Internet tomography, we therefore adopt the term *CRN tomography* in this paper. Let us start from the link-level parameter inference for the radio resource using active probing, which is also called radio resource tomography and provides critical information for wireless networks. It is worthwhile to note that the probing signal must operate under acceptable interference to the link or network, which suggests the need for the interference metric and impact the assessment of probing signals. Then, we can generalize this active probing to infer parameters at the network level by estimating/inferring the availability of opportunistic links for cooperative relays in CRN.

A. Link-Level Parameter Interference

Although many well-known passive techniques are introduced for the inference of link-level parameters in Section III-A, the passive techniques might not be applicable for some link-level parameters. For example, due to the hidden terminal problem, the CR-Tx would not actually know the interference to the PS receiver (PS-Rx) by passive listening to PS-Tx, whereas this information is usually a premise for the power control of CR-Tx [71]. Fortunately, active probing provides an alternative to infer these link-level parameters. A good example is the location awareness technique in [28] to achieve accuracy adaptation in both indoor and outdoor by the transmission of a stream of pulses, which is an excellent demonstration of the active probing for link-level parameters (distance among nodes). In this section, we develop active link-level CRN tomography to update available radio resource that is critical in CRN operation. Each CR-Tx has to determine the available radio resource of each cognitive link, which is defined as the maximum transmission power of CR-Tx with warrant of successful PS communication. With this information, many CRN operations can be established on top of it, such as the determination of routing paths, interference management, power control, and joint radio-resource allocation among the heterogeneous systems.

Under the following conditions, an active radio-resource-sensing algorithm is proposed to infer the interference from CR-Tx to PS-Rx and then the available radio resource of the cognitive link: 1) A feedback channel from PS-Rx to PS-Tx

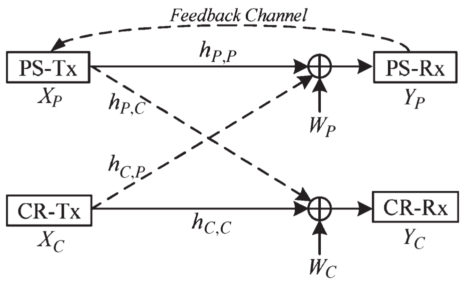

Fig. 5. Interference channel model.

in which PS-Tx can adjust its modulation and coding according to signal-to-interference-plus-noise ratio (SINR) information of PS-Rx and a predetermined adaptive modulation and coding (AMC) scheme [72] and 2) CR-Rx has the capability to detect the transmission parameters of PS-Tx.

1) System Model: Consider an interference channel model with a pair of PS-Tx/PS-Rx bearing a feedback channel and a pair of CR-Tx/CR-Rx as Fig. 5. The feedback channel common for orthogonal frequency-division multiple access is used for PS-Rx to deliver the channel quality information and for PS-Tx to adjust the modulation and coding. We assume the slowly time-varying channels, and hence, the channel power gains are virtually constants over the sensing interval. The received signals of PS-Rx can be written as $Y_P(t) = h_{P,P}X_P(t) + h_{C,P}X_C(t) + W_P(t)$, and the received signals of CR-Rx are $Y_C(t) = h_{P,C}X_P(t) + h_{C,C}X_C(t) + W_C(t)$, where $X_P(t)$ and $X_C(t)$ are the transmitted signals of PS-Tx and CR-Tx with signal power P_P and P_C, respectively; $h_{P,P}$, $h_{C,P}$, $h_{P,C}$, and $h_{C,C}$ are the complex channel gains with $g_{P,P} = |h_{P,P}|^2$, $g_{C,P} = |h_{C,P}|^2$, $g_{P,C} = |h_{P,C}|^2$, and $g_{C,C} = |h_{C,C}|^2$, respectively; and $W_P(t)$ and $W_C(t)$ are AWGNs with variance σ_P^2 and σ_C^2, respectively. The transmission power of CR-Tx P_C is inherently known by CR-Tx. We assume that there is no change in power control between PS-Tx and PS-Rx during operating duration, i.e., P_P is a constant. Furthermore, the channel power gains $g_{P,C}$ and $g_{C,C}$ can be estimated by conventional channel-estimation techniques in [73] and the references therein and can thus be regarded as known; $g_{P,P}$ and $g_{C,P}$ are unknown for CR-Tx and CR-Rx as a common condition in CR research.

Suppose that PS-Tx sends symbols with the modulation coding mode $M_P[i] \in \{M_0, \ldots, M_K\}$ in the ith frame. $M_P[i]$ is determined, following a predetermined AMC scheme. Here, M_0 represents the no-transmission mode. Assume that PS-Tx updates the modulation coding mode according to the SINR estimation result of the previous frame, i.e., the modulation coding mode of the $(i+1)$th frame $M[i+1]$ is determined by the AMC scheme

$$M[i+1] = \begin{cases} M_0, & \text{if } \hat{\gamma}_P[i] < l_1 \\ M_k, & \text{if } l_k \leq \hat{\gamma}_P[i] < l_{k+1} \\ M_k, & \text{if } \hat{\gamma}_P[i] > l_K \end{cases} \tag{13}$$

where $\hat{\gamma}_P[i]$ is the SINR estimation of PS-Rx in the ith frame, and l_j for $j = 1$ to K is the predetermined SINR threshold. From common synchronous operation assumption, CR-Tx is synchronous with PS-Tx to adjust the transmission power frame by frame. The real SINR of PS-Rx in the ith frame $\gamma_P[i]$ is defined as $\gamma_P[i] \equiv P_P \cdot g_{P,P}/P_C[i] \cdot g_{C,P} + \sigma_P^2$, where $P_C[i]$ is the transmission power of CR-Tx in the ith frame.

Note that, if mode M_0 is used, PS-Tx does not send data, and the outage of PS-Rx occurs. We define the harmless interference condition of PS-Rx as that the outage probability of PS-Tx should be guaranteed with the simultaneous transmission of CR-Tx. On the other hand, the transmission power of CR-Tx is commonly constrained as usual, and the maximum power is thus denoted as $P_{C,\mathrm{reg}}$. We define the radio resource of CR transmission as the maximum allowable transmission of CR-Tx under the harmless interference condition and formulate the radio-resource-sensing problem for cognitive link transmissions as follows:

Proposition 4.1 (Radio-Resource Sensing): The radio-resource sensing can be formulated as an optimization problem to find the maximum $P_C[i]$ subject to $P(M[i]{=}M_0|P_C[i]) \leq \rho$, where ρ is a given threshold, and $0 \leq P_C[i] \leq P_{C,\mathrm{reg}}$.

2) Cooperative AMC: Conventionally, the radio resource sensing problem is intuitively handled by the passive spectrum-sensing techniques to infer the interference from CR-Tx to PS-Rx using the safe-zone concept [74]. However, since the interference to PS-Rx is passively inferred by the received signal power level of PS-Tx in the ensemble probabilistic sense, there may be several problems [75]. Passive techniques inherently face the aforementioned problems, owing to the fact that the passive observations are completely executed by the reception of CR nodes (may be CR-Rx or CR-Tx [76]). Here, we introduce a novel iterative active method for radio resource of the cognitive link based on cooperative AMC between primary and secondary systems. Cooperative AMC combining the cooperative communication concept with conventional AMC scheme to iteratively determine the maximum $P_C[i]$. With CR-Rx reiterating the detection of the modulation coding mode from PS-Tx, the power of the probing signal increases to determine the maximum $P_C[i]$ that does not invoke the change of the modulation coding mode of PS-Tx. This iterative progress is constructed on the cooperative AMC, as the CR Tx-Rx pair cooperates to adjust the transmission power according to the AMC scheme of PS-Tx. The operation of the radio resource sensing algorithm with cooperative AMC is summarized as Algorithm 2.

Algorithm 2 Radio-Resource-Sensing Algorithm With Cooperative AMC

1: Initialize: $k = 1$ and $I_C[1] = \Delta I_C$.
2: Detect the modulation coding mode of PS-Tx, which is denoted as M_q. If $q = 1$, end; otherwise, go to step 3.
3: Transmit the probing signal with power $I_C = I_C[k]$.
4: Wait for a period τ.
5: Detect the modulation coding mode of PS-Tx, which is denoted as M_r. If $q - r = 1$, go to step 7. If $q - r \geq 2$, end. Otherwise, $I_C[k] = I_C[k] + \Delta I_C[k]$.
6: If $I_C[k] \geq P_{C,\mathrm{reg}}$, the maximum allowable transmission power $P_{C,\max} = P_{C,\mathrm{reg}}$, end; otherwise, $k = k + 1$, and go to step 4.
7: The maximum allowable transmission power $P_{C,\max} = \gamma_{\mathrm{sw}} \cdot I_C/l_1$, end.

With the probing transmission of CR-Tx, CR-Rx needs to detect the modulation coding mode of PS-Tx. The modulation coding mode of PS-Tx may directly be decoded by the pilot or the header of frames radiated from PS-Tx. If this approach is not available, the modulation coding mode should be detected according to the received traffic signals of CR-Rx. The detection of modulation has been well studied in modulation classification, as an intermediate step between signal detection/interception and signal demodulation [77]–[79]. The multi-purpose detection of the probing signal and PS-Tx signals could be facilitated. After demodulation, the detection of coding from the traffic signals can be accomplished using the frame structure that is characteristic for the frames with synchronization words as [80].

3) Impact of Imperfect SINR Estimation: Considering the robustness of our algorithm, there would be two kinds of radio resource sensing error: 1) the detection error of the modulation coding mode and 2) the imperfect SINR estimation of PS-Rx. Note that we assume that the step size ΔI_C is small enough to smoothly achieve $\gamma_{\rm sw}$ and, thus, $P_{\rm sw}$. The detection error of the modulation coding mode can be alleviated with longer observation time and effective detection of CR-Tx. However, the SINR estimation error happens at (legacy) PS-Rx and cannot be mitigated by the effort of CR nodes. When a long observation time is available to perfectly identify the modulation coding mode of PS-Tx, the impact of imperfect SINR estimation of PS-Rx is particularly considered as the upper bound performance of our proposed algorithm. Many SINR estimation techniques have been proposed and compared in [81]. The SINR estimation error using the ML estimate, which calculates the ML estimate of the received signal amplitude and the ML estimate of the noise power, is computed in [82]. Following these results, the impact of imperfect SINR estimation on the outage probability of PS-Rx can therefore be evaluated as in [75].

4) Performance Evaluation: We consider several assumptions for the simulations of performance evaluation: 1) The feedback channel between PS-Tx and PS-Rx is perfect. 2) The modulation coding mode can accurately be known. $g_{\rm PC}$ and $g_{\rm CC}$ are accurately estimated by the secondary system. 3) $P_{\rm sw}$ can perfectly be achieved. 4) The noise power is small, compared with interference power, and ignorable for SINRs of interest.

Under these assumptions, the dominating error in determining $P_{C,\max}$ results from the SINR estimation error of PS-Rx. Without loss of generality, the SINR estimation result (in decibel scale) of the PS-Rx is modeled as a random variable $\hat{\gamma}$ with Gaussian distribution, where $E\{\hat{\gamma}\} = \gamma$ is the real SINR value and $\sigma_{\rm SINR}$ is the standard deviation. The simulation environment is shown in Fig. 6. The outage probability of PS-Rx for the active radio resource tomography algorithm is shown in Fig. 7. Note that $P_{o,PS}$ is affected by δ and the accuracy of SINR estimation of PS-Rx but not by the parameters of the propagation model since our algorithm is actually sensing the interference at PS-Rx.

For the purpose of comparison, we take the power-scaling technique in [74] with $\Delta = 71.6$ dB and $\mu = 1$ dB and suppose that the distance between PS-Tx and CR-Tx can perfectly be estimated; thus, CR can determine the maximum transmission power. We model the propagation as a path-loss channel with the channel power gain as $G(r) = r^{-\alpha}$, where γ is the distance between the transmitter and the receiver, and α is the path-loss exponent. Assume that the system parameters are $P_P = 10$ dBm, $\Delta = 71.6$ dB, $\mu = 1$ dB, $\sigma^2 = -70$ dBm, and $l_1 = 8.4$ dB.

At the PS-Rx side, Fig. 8 shows the average SINR of the PS-Rx when it moves along the line from PS-Tx to CR-Tx. The location 0 m (i.e., origin) is corresponding to the PS-Tx.

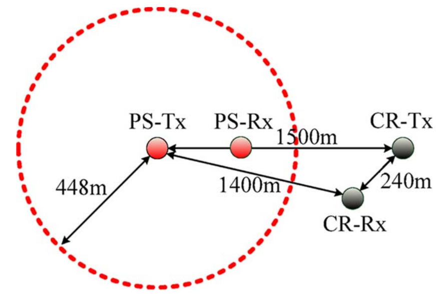

Fig. 6. Simulation environment.

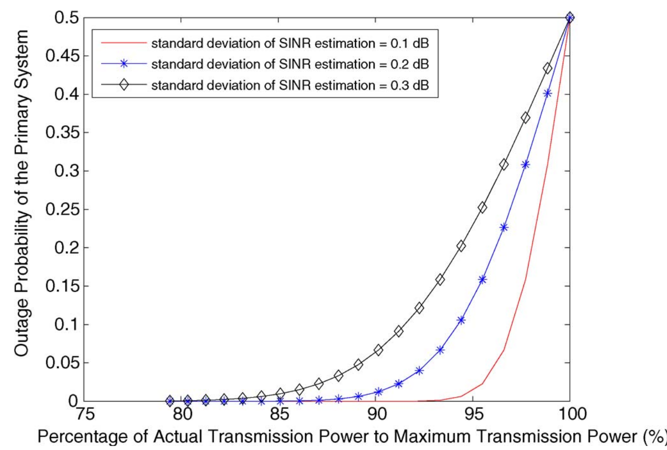

Fig. 7. Outage probability of PS for the active radio resource tomography algorithm.

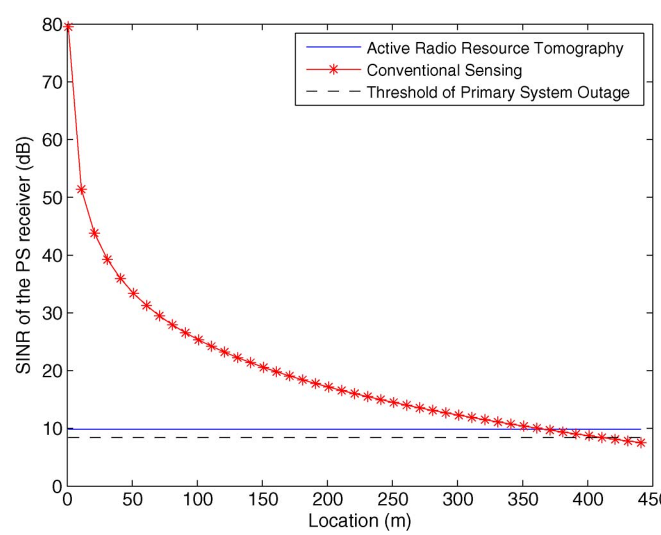

Fig. 8. SINR of PS-Rx according to the PS-Rx location with $\delta = 0.8675$ and $P_C = 6.1207$ dBm.

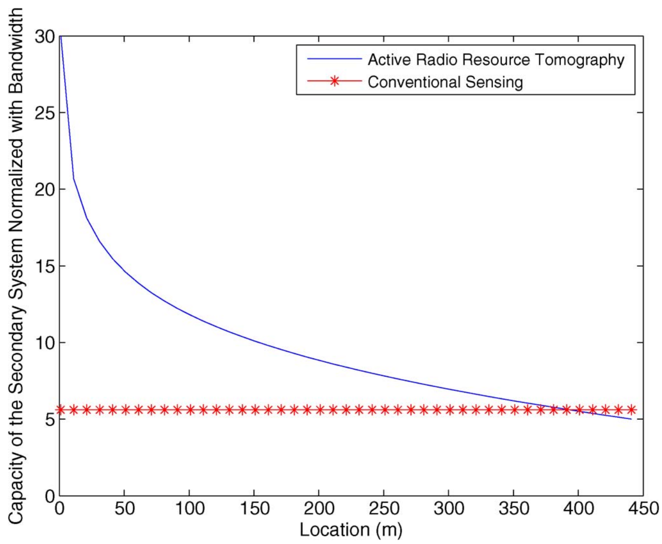

Fig. 9. Normalized capacity of the secondary system according to the PS-Rx location with $\delta = 0.8675$ and $P_C = 6.1207$ dBm.

According to these parameters, we observe from Fig. 8 that the outage of PS-Rx occurs in conventional sensing but does not occur in our algorithm, when the location is greater than 410 m or so. In the mean time, the normalized capacity of the secondary system is defined as $\log_2(1 + \mathrm{SINR})$. A significant improvement of the normalized capacity is achieved in the active tomography algorithm as Fig. 9, because our algorithm actually probes and utilizes the channel between PS-Tx and CR-Rx rather than simply assuming the worst-case scenario. Please note that CR adopting the active radio-resource tomography can, in real time, adapt to the environment without *a priori* information, such as the channel model and its parameters.

Remarks: In the radio resource tomography/sensing, we only use the AMC information of PS and assume constant power for PS during the period. The cooperative AMC is proposed to combine AMC and cooperative communication. We successfully demonstrate that the active radio-resource tomography can support real-time adaptation to dynamic environments with no *a priori* information from radio channels. The power control of PS can be another useful tool to infer the radio resource of the cognitive link. In [83], the hidden power-feedback loop is exploited to estimate the effective channel power gain from CR-Tx to PS-Rx as another example for active link-level probing.

B. Network-Level Parameter Inference

For CRN, it is difficult to guarantee the quality of service (QoS) for end-to-end transmission due to the CRN nature link, the opportunistic links in the link level, or the heterogeneous system packet queue in the network level. The cooperative opportunistic relays, which exploit neighboring nodes to cooperative relay packets, could increase the reliability of transmission by multiple end-to-end paths, further improve the network throughput [11], [14], and provide the most general scope in CRNs (than those CRNs who cannot deal with cooperative opportunistic relays); however, no mature study is developed. In this section, we present the active network-level CRN tomography for success probability estimation regarding cooperative opportunistic relays, which might also be useful to enhance existing standard efforts or general-sense CRN. The cooperative opportunistic relays of CRN networking operations through neighboring (CR) nodes always require *a priori* knowledge or estimation of such cooperative relay node-to-node availability to implement routing and flow control [66], etc. This node-to-node availability, which embraces the link availability among one-hop neighboring nodes, may relate to radio resource, CR mechanism, and trust [21]. Because of the dynamic and opportunistic transmission nature of CRN, the guaranteed QoS control provides an intellectual challenge [23]. Given the statistics of the node-to-node availability, statistical QoS control [84] can be considered as an alternative way for end-to-end services in CRN operations. To infer such *a prior* knowledge or estimation of node-to-node availability associated with a cooperative relay, we may observe the history and statistics of successful packet transportation (or delivery probability) over a specific cooperative relay path. Since there involves packet transmissions (either implicit traffic packets or explicit probing packets) usually for network layer functions, we categorize this approach as active CRN tomography at the network level.

The heterogeneous and largely unregulated structure of the Internet renders tasks such as dynamic routing, optimized service provision, service-level verification, and detection of anomalous/malicious behavior extremely challenging since the Internet is a massive distributed network [40]. Internet tomography deals with the problem of extracting hidden information from active or passive traffic measurements falls in the realm of statistical inverse problems. Many topics are well discussed in Internet tomography, such as the estimation of link loss rates, estimation link delay distributions, and topology identification. While Internet tomography is a well-known research, in this paper, we systematically explore appropriate CRN tomography for smooth CRN operations at the link and network levels, which is beyond Internet tomography due to the shared radio resource and stochastic radio links to open a new dimensional research via statistical inference or learning algorithms. There exists much research in conventional Internet/network tomography to deal with the packet loss rate. For active methodology in Internet tomography, the estimate of network performance based on end-to-end measurements can be multicast transmission based [85] or unicast probing based [86]. Furthermore, several kinds of random tools in Internet tomography for different network modeling and environment are proposed [87]–[89]. Due to the shared radio resource among coexisting primary/secondary systems and the random radio links, in this section, we consider the success probability estimation in CRN tomography beyond the scope of Internet tomography and start with a typical scenario with a set of possible cooperative relay paths. Under the operations of coexisting communication links, the source node estimates the success probability of packet transmission according to the historical record from the reception of the destination node. Both traffic types of the deterministic packet arrival and the Poisson packet arrival from the source node will be illustrated.

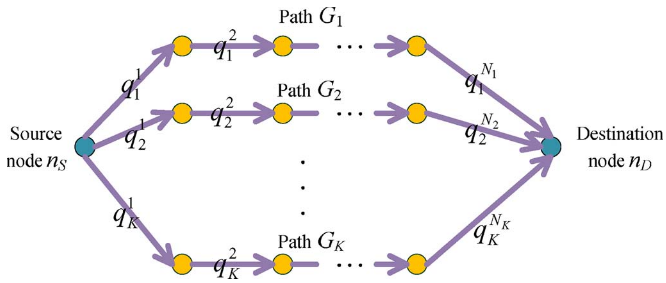

Fig. 10. Cooperative opportunistic relay network.

1) System Model: Consider the CRN topology, as shown in Fig. 10, where a source node n_S transmits packets to a destination node n_D through K possible relay paths G_j, $j = 1$, to K, where there are N_j links numbered as q_j^n, $n = 1$, and to N_j in the G_j relay path. That is, the G_j relay path has N_j links. Let the successful transmission probability in the q_j^n link be $P_S^{n,j}$, which is chosen beforehand according to the uniform distribution on the interval [0, 1] and unchanged in thereafter packet transmissions. Assume that the packets are transported in a slotted network between the source node and the destination node, respectively, with time interval Δt_j in one time slot for the relay path G_j, and the propagation delay of G_j relay path D_j is constant. The destination node can observe the packet reception in M time slots (and, thus, $M\Delta t_j$ observation time for the relay paths G_j), and the source node can explicitly/implicitly collect such information while we assume reliable collection hereafter. It is reasonable to assume that the destination node knows the relay path of each received packet. That is, suppose that the probabilities $\{P_S^{n,j}\}_{n=1}^{N_j}$ are independently determined for each relay path G_j.

2) One-Hop Transmission for a Specific Path: The one-hop transmission for a specific path G_j, where $N_j = 1$, can be referred in [22]. Considering the deterministic packet arrival, we suppose that the source node transmits one packet by the routing path G_j to the destination node (and, thus, the packet rate is fixed in $1/\Delta t_j$) in each time slot. The reception state of the ith transmission by the relay path G_j is Bernoulli distributed with expected value P_S^j, i.e., with probability P_S^j equal to 1 and probability $(1 - P_S^j)$ equal to 0. With mean square error cost function, the Bayes estimator becomes

$$\hat{P}_{S,MS}^j(\boldsymbol{r}) = \frac{q_j + 1}{M + 2}. \tag{14}$$

On the other hand, with uniform cost function, the Bayes estimator becomes

$$\hat{P}_{S,\mathrm{UNF}}^j(\boldsymbol{r}) = \frac{q_j}{M}. \tag{15}$$

$\hat{P}_{S,MS}^j(\boldsymbol{r})$ coincides with the result of Laplace's rule of succession that, if the destination observes that the first M transmissions in q_j succeed, then the next transmission from the source node by the jth relay path will be a success with probability $(q_j + 1)/(M + 2)$, which is a well-known inference method for binomial proportion.

On the other hand, in the Poisson packet-arrival case, the packets arrive on G_j as a Poisson process having rate λ_j. Therefore, in each time slot, the probability of no packet to be transmitted is $P_N^j = e^{-\lambda_j \Delta t_j}$. Assume that $\lambda_j \Delta t_j$ is small enough, which results in the negligible probability that more than one packet arrives within one time slot. Hence, we can only consider the probability that one packet arrives as $P_Y^j \cong 1 - e^{-\lambda_j \Delta t_j}$ and no packet arrives as P_N^j. Define an indicator function $\mathbb{I}_j^R[i]$ to represent the reception result from the jth relay path in the ith observation by G_j at the destination node that $\mathbb{I}_j^R[i]$ is equal to 1 with successful reception and equal to 0 with no reception. Let $s_j = \sum_{i=1}^{M} \mathbb{I}_j^R[i]$ and the observation $\boldsymbol{r}$ be $\boldsymbol{r} = [\mathbb{I}_j^R[1], \mathbb{I}_j^R[2], \ldots, \mathbb{I}_j^R[i]]^T$. If the propagation delay D_j is known, the source node can know the root cause of no reception resulting from no transmission from the source node or transmission failure. According to the historical observations of the destination node, $\hat{P}_{S,MS}^j(\boldsymbol{r})$ becomes

$$\hat{P}_{S,MS}^j(\boldsymbol{r}) = \frac{s_j + 1}{M_j + 2} \tag{16}$$

where M_j is the number of actual transmissions, and $\hat{P}_{S,MS}^j(\boldsymbol{r})$ becomes

$$\hat{P}_{S,\mathrm{UNF}}^j(\boldsymbol{r}) = \frac{s_j}{M_j}. \tag{17}$$

On the other hand, if the propagation delay is unknown, the source node can only know the statistics in certain M observations of the destination node. $\hat{P}_{S,MS}^j(\boldsymbol{r})$ becomes

$$\hat{P}_{S,MS}^j(\boldsymbol{r}) = \frac{s_j + 1}{M + 2} \frac{1}{P_Y^j} \frac{I_{P_Y^j}(s_j + 2, M - s_j + 1)}{I_{P_Y^j}(s_j + 1, M - s_j + 1)} \tag{18}$$

where $I_x(a, b)$ is the regularized incomplete beta function [90], and

$$\hat{P}_{S,\mathrm{UNF}}^j(\boldsymbol{r}) = \frac{s_j}{M P_Y^j}. \tag{19}$$

When $P_Y^j = 1$, due to the fact that $I_1(a, b) = 1$ for any a and b, (18) and (19) are degenerated to the results of $\hat{P}_{S,MS}^j(\boldsymbol{r}) = (q_j + 1)/(M + 2)$ and $\hat{P}_{S,\mathrm{UNF}}^j(\boldsymbol{r}) = q_j/M$ as (14) and (15) in the result of Laplace's rule of succession. Note that (18) and (19) also give a way to adapt the estimators according to the traffic status of the source node with the parameter λ_j of the Poisson process.

3) Multihop Transmission for a Specific Path: Consider a specific relay path G_j with multiple links, where $N_j \geq 2$. That is, the transmissions from the source to the destination are through multiple hops. The *a priori* probability density function (pdf) of P_S^j, i.e., $f(P_S^j)$, becomes $\prod_{n=1}^{N_j} f(P_S^{n,j})$ since $\{P_S^{n,j}\}_{n=1}^{N_j}$ are independent with uniform distribution on the interval [0, 1]. Let $Q_j = \ln P_S^j = \sum_{n=1}^{N_j} \ln P_S^{n,j}$. Thus, $(-\ln P_S^{n,j})$ has an exponential distribution with parameter $\lambda = 1$, and $X = (-Q_j)$ follows an Erlang distribution with the pdf:

$$f(xN_j, 1) = \frac{x^{N_j - 1} e^{-x}}{(N_j - 1)!}. \tag{20}$$

Therefore, based on the fact that $P_S^j = e^{Q_j} = e^{-X}$, we can express the pdf of P_S^j as

$$f(P_S^j) = \frac{\left(-\ln P_S^j\right)^{N_j-1}}{(N_j-1)!}. \quad (21)$$

Now we consider the asymptotical behavior of the pdf of P_S^j. According to the *Central Limit Theorem*, when N_j becomes large, the distribution of Q_j tends to the normal distribution $\mathbb{N}(-N_j, N_j)$. Therefore, the *a priori* pdf of P_S^j tends to a lognormal distribution

$$f\left(P_S^j\right) \to \frac{1}{P_S^j N_j \sqrt{2\pi}} e^{-\frac{\left(\ln(x)-N_j\right)^2}{2(N_j)^2}} \quad (22)$$

as the number of links N_j becomes large.

The results of (21) and (22) provide the exact and asymptotical descriptions of pdf of P_S^j. However, with such *a priori* information, Bayes estimators are hard to find with closed form. In this case, by the *Weierstrass Approximation Theorem*, we can always find a polynomial to approximate a continuous function on a closed and bounded interval to any desired degree of accuracy. Therefore, let $f(P_S^j)$ be represented by $\sum_{i\geq 0} a_i (P_S^j)^i$, such that the approximation error is less than an arbitrarily small ϵ. The weights a_i arise from the polynomial approximation of the prior density $f(P_S^j)$, which can be calculated through a Taylor series representation [91]

$$f(x) = \sum_{n=0}^{\infty} \frac{f^{(n)}(a)}{n!}(x-a)^n \quad (23)$$

where $f^{(n)}(a)$ denotes the nth derivative of f evaluated at the point a.

For the deterministic packet arrival case, we have the following lemma:

Lemma 4.1: The Bayes estimator with mean square error cost function becomes

$$\hat{P}_{S,MS}^j(\boldsymbol{r}) = \frac{\sum_{i\geq 0} a_i (q_j+i+1)!/(M+i+2)!}{\sum_{t\geq 0} a_t (q_j+t)!/(M+t+1)!} \quad (24)$$

and the Bayes estimator with uniform cost function estimator becomes

$$\hat{P}_{S,\mathrm{UNF}}^j(\boldsymbol{r}) = \arg_{(P_S^j)^* \in \boldsymbol{P}_S^j} \max f\left(\left(P_S^j\right)^* \middle| \boldsymbol{r}\right) \quad (25)$$

where $\boldsymbol{P}_S^j$ is the solution set of the polynomial equation

$$\sum_{i\geq 0} \left[a_{i+1}(q_j+i+1) - a_i(M+i)\right] \left(P_S^j\right)^{i+1} = 0. \quad (26)$$

Proof: The *a posteriori* pdf of P_S^j can be expressed as

$$f\left(P_S^j | \boldsymbol{r}\right) = \frac{\sum_{i\geq 0} a_i \left(P_S^j\right)^{q_j+i} \left(1-P_S^j\right)^{M-q_j}}{\sum_{t\geq 0} a_t (q_j+t)!(M-q_j)!/(M+t+1)!}. \quad (27)$$

■

On the other hand, for the Poisson packet-arrival case, we can derive the following lemmas:

Lemma 4.2: If the propagation delay is known

$$\hat{P}_{S,ML}^j(\boldsymbol{r}) = \frac{\sum_{i\geq 0} a_i (s_j+i+1)!/(M_j+i+2)!}{\sum_{t\geq 0} a_t (s_j+t)!/(M_j+t+1)!} \quad (28)$$

$$\hat{P}_{S,\mathrm{UNF}}^j(\boldsymbol{r}) = \arg_{(P_S^j)^* \in \boldsymbol{P}_S^j} \max f\left(\left(P_S^j\right)^* \middle| \boldsymbol{r}\right) \quad (29)$$

where $\boldsymbol{P}_S^j$ is the solution set of the polynomial equation

$$\sum_{i\geq 0} \left[a_{i+1}(s_j+i+1) - a_j(M_j+i)\right] \left(P_S^j\right)^{i+1} = 0. \quad (30)$$

Lemma 4.3: If the propagation delay is unknown, $\hat{P}_{S,MS}^j(\boldsymbol{r})$ becomes (31), shown at the bottom of the page, where $\boldsymbol{P}_S^j$ is the solution set of the polynomial equation

$$\sum_{i\geq 0} \left[a_{i+1}(s_j+i+1) - a_i\left(s_j+i+P_Y^j(M_j+i)\right)\right] \left(P_S^j\right)^i = 0. \quad (32)$$

Proof: The *a posteriori* pdf of P_S^j can be expressed as

$$f\left(P_S^j | \boldsymbol{r}\right) = \frac{\sum_{i\geq 0} a_i \left(P_Y^j\right)^{-i} \left(P_S^j P_Y^j\right)^{s_j+i} \left(1-P_S^j P_Y^j\right)^{M-s_j}}{\sum_{t\geq 0} a_t \left(P_Y^j\right)^{-(t+1)} B\left(P_Y^j s_j+t+1, M-s_j+1\right)}. \quad (33)$$

■

Multihop Transmission for Multiple Paths: Considering multiple paths, the correlations among paths are an inevitable challenge of CRN. The success probability of paths is correlated due to the sharing of spectrum of the primary and cognitive links or the common links of relay paths.

When primary and secondary systems share the same frequency band, the transmissions of primary and cognitive links would be correlated. We can use a two-class priority queue to mathematically model the behaviors and interactions of the primary and secondary system transmissions. Since the cognitive links are granted to opportunistically exploit unused frequency bands without interfering with primary links, cognitive links should vacate the frequency band when detecting the arrival of primary transmissions and restart to exploit the spectrum hole again after detecting the completion of primary transmissions. By considering the opportunistic nature of

$$\hat{P}_{S,MS}^j(\boldsymbol{r}) = \frac{s_j+1}{M+2}\frac{1}{P_Y^j} \times \frac{\sum_{i\geq 0} a_i \left(P_Y^j\right)^{-(i+1)} I_{P_Y^j}(s_j+i+2, M-s_j+1)}{\sum_{t\geq 0} a_t \left(P_Y^j\right)^{-(t+1)} I_{P_Y^j}(s_j+t+1, M-s_j+1)} \quad (31)$$

cognitive links, preemptive-repeat-identical policy for cognitive links (i.e., lower priority item) should be adopted in the priority queue. In this discipline, primary transmission arrivals during the secondary system transmission are regarded as an interrupt. After the interrupt is cleared, a service period of the same duration as that interrupted is commenced again. Consider that there exists a kind of primary packets of class 1 and a kind of secondary packets of class 2, which arrive as a Poisson process with arrival rates λ_1 and λ_2 into exponential servers with service rates μ_1 and μ_2.

Let W_1 denote the total time that a class-1 arriving packet spends in the system, which includes waiting time in queue W_1^q and service time W_1^s. Let $W_1(t)$ denote the cumulative distribution function (cdf) of W_1. Under the preemptive service discipline, the presence of packets of class 2 does not influence the stochastic law of class-1 process. Thus, W_1 can easily be computed by considering that the class-2 packet is not present in the system, and W_1 is an exponential random variable with mean $1/(\mu_1 - \lambda_1)$. That is

$$W_1(t) = 1 - e^{-(\mu_1-\lambda_1)t}. \tag{34}$$

Regarding the class-2 packet, let W_2 denote its total time in the system, which includes waiting time in queue W_2^q and completion time W_2^c. Note that the completion time W_2^c is defined as the duration of period that elapses between the instant at which the service of a class-2 packet begins and the instant at which that packet departs [92]. It is obvious that W_2^c is the sum of service time for the CR packet and any additional durations resulting from PS arrivals.

However, due to the preemptive-repeat-identical principle, the cdf of W_2 is more complicated than that of W_1, and we separately derive W_2^q and W_2^c for better representation. Let $w_2^c(\cdot)$ ($w_2^q(\cdot)$) and $L_2^c(s)$ ($L_2^q(s)$) be the pdf of the completion time (waiting time in queue) and the Laplace transform of the function, respectively. From [93], $L_2^c(s)$ can be derived as

$$L_2^c(s) = \frac{e^{-(s+\lambda_1+\mu_2)}(s+\lambda_1)}{s+\lambda_1-\lambda_1\left(e^{-(s+\mu_1)}\right)\left(1-e^{-(s+\lambda_1+\mu_2)}\right)} \tag{35}$$

and $L_2^q(s)$ as

$$L_2^q(s) = \left[\frac{s\left(1-\lambda_1 E\left[w_2^c\right]\right)L_2^c(s)}{s-\lambda_2+\lambda_2 L_2^c(s)}\right] \times \left[\frac{s+\lambda_1-\lambda_1 e^{-(s+\mu_1)}}{s(1+\lambda_1\mu_1)}\right] \tag{36}$$

where $E[w_2^c]$ is the first moment, given the differentiation of (35), i.e.,

$$\begin{aligned} E\left[w_2^c\right] &= (-1)\left[\frac{dL_2^c(s)}{ds}\right]\Bigg|_{s=0} \\ &= \left\{\frac{1-E[e^{-\lambda_1 s}]}{E[e^{-\lambda_1 s}]}\right\}\left(\mu_1+\frac{1}{\lambda_1}\right). \end{aligned} \tag{37}$$

It is obvious that the completion time W_2^c is affected by the primary transmission arrivals since it consists of the secondary system packet-service time and the service times of PS packets that arrive while the primary or secondary system packet is in service. Regarding the waiting time W_2^q, (36) indicates that $W_2^q(\cdot)$ is the convolution of two distributions, and the first distribution is same as the waiting time distribution for a single server with Poisson input of density λ_2 and a service time distribution of $W_2^c(\cdot)$. Since it is reasonable to assume that each packet has its own "Time to Live," we can observe that the successful transmission probabilities of primary and cognitive links are likely to be correlated in this case. The simulation of the correlation between $\Pr[W_1 > T]$ and $Pr[W_2 > T]$ with different μ_2 is shown in Fig. 11, where the correlation of the delay of class-1 and class-2 packets is observed.

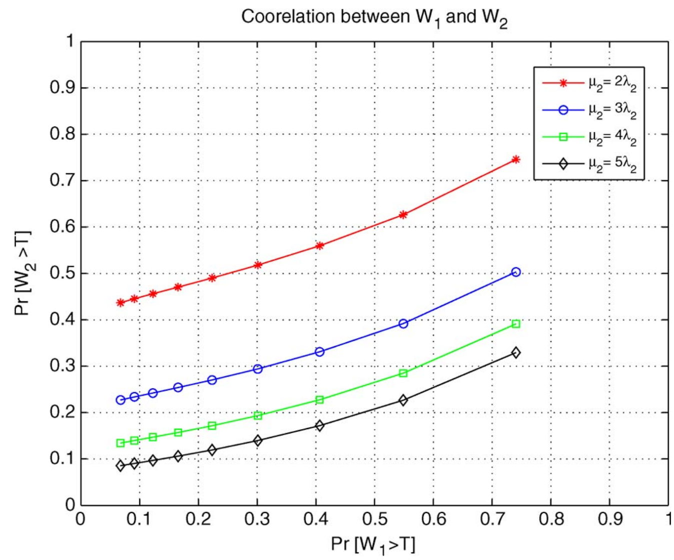

Fig. 11. Correlation between $\Pr[W_1 > T]$ and $\Pr[W_2 > T]$ with different μ_2's.

Another reason causing the correlations among the successful transmission probabilities of paths would be the common links of relay paths. Consider two relay paths G_i and G_j with N_i and N_j links, respectively, where there are K_c common links for G_i and G_j. The success statistics of all links are assumed to be independently and uniformly chosen from interval [0, 1] before packet transmission. Therefore, we have the successful transmission probabilities of the relay path G_i, $P_S^i = \prod_{k=1}^{K_c} P_{\text{common}}^k \cdot \prod_{m=1}^{N_i-K_c} P'_m$, and the relay path G_j, $P_S^j = \prod_{k=1}^{K_c} P_{\text{common}}^k \cdot \prod_{p=1}^{N_j-K_c} P''_p$, where P_{common}^k is the successful transmission probability of the kth common link. The covariance of P_S^i and P_S^j can consequently be expressed as

$$\begin{aligned} C_{P_S^i P_S^j} &= E\left\{P_S^i P_S^j\right\} - \eta_{P_S^i}\eta_{P_S^j} \\ &= E\left\{\prod_{k=1}^{K_c}\left[p_{\text{common}}^k\right]^2\right\} \\ &\quad \cdot E\left\{\prod_{m=1}^{N_i-K_c} P'_m \prod_{p=1}^{N_j-K_c} P''_P\right\} - (\eta_{P_S})^{N_i+N_j} \\ &= \prod_{k=1}^{K_c} E\left\{\left[P_{\text{common}}^k\right]^2\right\} \cdot (\eta_{P_S})^{N_i+N_j-2K_c} \\ &\quad - (\eta_{P_S})^{N_i+N_j} \\ &= \left(E\left\{\left[P_{\text{common}}^k\right]^2\right\}\right)^{K_c} \cdot (\eta_{P_S})^{N_i+N_j-2K_c} \\ &\quad - (\eta_{P_S})^{N_i+N_j} \end{aligned} \tag{38}$$

where $\eta_{P_S^t}$ is the mean of P_S^t for all t, and we neglect the index t since P_S^t for all t are i.i.d. random variables with the same mean. It can easily be verified that (38) is equal to 0 if and only if $K_c = 0$. Therefore, the sharing of common links results in the correlation of paths.

In the multihop-transmission and multiple-path case, the observation $\boldsymbol{r}$, which is given by $\boldsymbol{r} = [q_1, q_2, \ldots, q_K]^T$, is a $K \times 1$ vector, where q_j is the successes in M transmissions of relay path G_j. Since the closed form is hard to reach, we consider the asymptotic behavior of the success probability estimation in the following.

Since $Q_j = \ln P_S^j = \sum_{n=1}^{N_j} \ln P_S^{n,j}$ and the distribution of Q_j tends to the normal distribution $\mathbb{N}(-N_j, N_j)$ with large N_j, the joint multivariate distribution of the random vector $\boldsymbol{Q} = [Q_1, Q_2, \ldots, Q_K]^T$, which is the *a priori* distribution of $\boldsymbol{Q}$, can be written as the multivariate normal distribution with pdf, i.e.,

$$f(\boldsymbol{Q}) = \frac{1}{(2\pi)^{K/2}|\boldsymbol{C}_Q|^{1/2}} e^{(\boldsymbol{Q}-\boldsymbol{\mu})^T \boldsymbol{C}_Q^{-1}(\boldsymbol{Q}-\boldsymbol{\mu})/2} \tag{39}$$

where $\boldsymbol{C}_Q$ is the covariance matrix where the (i, j)th element C_{ij} is the covariance of Q_i and Q_j, and $\boldsymbol{\mu} = [\eta_{P_S^1}, \eta_{P_S^2}, \ldots, \eta_{P_S^K}]^T$ is the mean vector. We suppose that the covariance matrix can be estimated by the Pearson product-moment correlation coefficient [94] with historical measurements of $\{Q_j\}_{j=1}^K$.

For deterministic packet arrival, we can write the *a posteriori* pdf of $\boldsymbol{Q}$ as

$$f(\boldsymbol{Q}|\boldsymbol{r}) = \frac{\prod_{i=1}^K (e^{Q_i})^{q_i}(1 - e^{Q_i})^{N_i - q_i} \cdot f(\boldsymbol{Q})}{\int_{\boldsymbol{Q}} \prod_{k=1}^K (e^{Q_k})^{q_k}(1 - e^{Q_k})^{N_k - q_k} \cdot f(\boldsymbol{Q}) d\boldsymbol{Q}}. \tag{40}$$

Thus, the Bayes estimators with mean square error cost function $\hat{P}_{S,MS}^j(\boldsymbol{r})$ can be expressed as

$$\hat{P}_{S,MS}^j(\boldsymbol{r}) = e^{\hat{Q}_{\mathrm{MS}}^j} \tag{41}$$

where

$$\hat{Q}_{\mathrm{MS}}^j = \frac{\int_{\boldsymbol{Q}} Q_j \prod_{i=1}^K (e^{Q_i})^{q_i}(1 - e^{Q_i})^{N_i - q_i} \cdot f(\boldsymbol{Q}) d\boldsymbol{Q}}{\int_{\boldsymbol{Q}} \prod_{k=1}^K (e^{Q_k})^{q_k}(1 - e^{Q_k})^{N_k - q_k} \cdot f(\boldsymbol{Q}) d\boldsymbol{Q}}. \tag{42}$$

On the other hand, with uniform error cost function, $\hat{P}_{S,\mathrm{UNF}}^j(\boldsymbol{r})$ can be obtained by

$$\hat{P}_{S,\mathrm{UNF}}^j(\boldsymbol{r}) = e^{\hat{Q}_{\mathrm{UNF}}^j} \tag{43}$$

where

$$\hat{Q}_{\mathrm{UNF}}^j = \arg\max_{Q_j} f(Q_j|\boldsymbol{r}). \tag{44}$$

For the Poison packet arrival case with known propagation delay, the estimation results can easily be reduced into a similar form as (40). On the other hand, for the case with unknown propagation delay, the *a posteriori* pdf of $\boldsymbol{Q}$ can be rewritten as

$$f(\boldsymbol{Q}|\boldsymbol{r}) = \frac{\prod_{j=1}^K (e^{Q_j})^{q_j}(1 - e^{Q_j})^{N_j - q_j} P_Y^j \cdot f(\boldsymbol{Q})}{\int_{Q} \prod_{j=1}^K (e^{Q_j})^{q_j}(1 - e^{Q_j})^{N_j - q_j} P_Y^j \cdot f(\boldsymbol{Q}) d\boldsymbol{Q}}. \tag{45}$$

Again, the Bayes estimators $\hat{P}_{S,MS}^j(\boldsymbol{r})$ and $\hat{P}_{S,\mathrm{UNF}}^j(\boldsymbol{r})$ can be obtained according to (45).

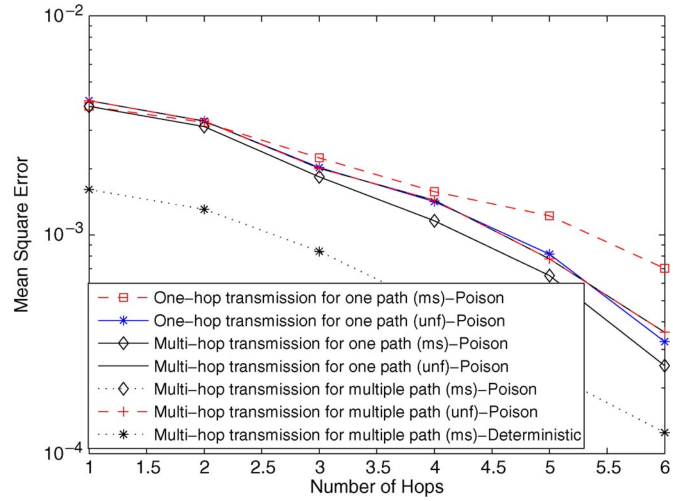

Fig. 12. Three paths without correlations of successful probabilities.

4) Numerical Results: We consider three paths without and with correlations, respectively. For the case without correlations, Fig. 12 shows the mean square error with respect to the number of hops, with the Poison packet arrivals, while the multihop multipath estimator of the deterministic packet arrival is a lower bound benchmark due to inherent deterministic information in each time slot.

We set the time interval as 1 s, i.e., $\Delta t_j = 1(s)$. According to [95], a reasonable parameter for message arrival is 0.15 message/s, with each message including 10–20 packets. Since $P_Y^j \cong 1 - e^{-\lambda_j \Delta t_j}$, we set the parameters P_Y^j as $P_Y^1 = 0.85$, $P_Y^2 = 0.9$, and $P_Y^3 = 0.95$ as a realistic environment consideration. We can find that, when the number of hops increases, the multihop estimators is likely to outperform the one-hop estimators with the same cost function since the multihop estimators consider a more accurate *a priori* distribution $f(\boldsymbol{Q})$, which demonstrates the effectiveness of the proposed methodology.

For the simulation with correlations of successful probabilities of paths, we consider the correlation matrix

$$\mathbf{C_Q} = \begin{bmatrix} 1.0 & 0.7 & 0.6 \\ 0.7 & 1.0 & 0.9 \\ 0.6 & 0.9 & 1.0 \end{bmatrix}. \tag{46}$$

In this case, Fig. 13 shows the mean square error with respect to the number of hops. We set the same parameters P_Y^j as in the case without correlation as $P_Y^1 = 0.85$, $P_Y^2 = 0.9$, and $P_Y^3 = 0.95$. Since our multihop multipath estimators take the correlation among successful probabilities of paths into consideration, we can observe that the performance of the multihop multipath estimators of Poison packet arrivals is better than that of the other estimators in the case with correlations.

From numerical results in Figs. 12 and 13, the mean square error of each estimator reduces with the increase in the number of hops. According to (21), as the number of hops N_j increases, the mean of the distribution of P_S^j can be written as e^{-N_j}, which tends to 0, and $f(P_S^j)$ becomes central. Therefore, P_S^j is more likely to be generated from a smaller region, which would result in the lower mean square error of a specific estimator of the Poison packet arrivals in ensemble average sense, because the estimate results are nearer the real value.

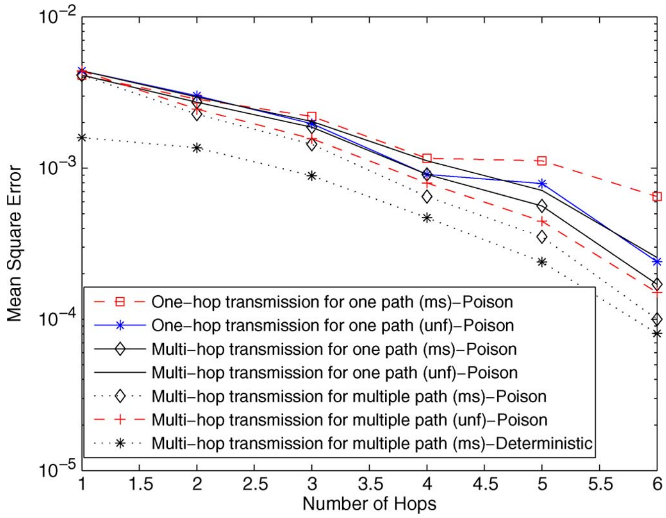

Fig. 13. Three paths with correlations of successful probabilities.

5) Application: Sections IV-B2–4 offer simple estimators for the inference of success probability $\hat{\boldsymbol{P}}_S = [\hat{P}_S^1, \hat{P}_S^2, \ldots, \hat{P}_S^K]^T$ in different traffic types (deterministic and Poisson packet arrival) of the source node, which are accomplished according to the historical observations of receptions at the destination node. They can easily be extended to many tomography application scenarios for upper layer CRN functions as follows:

Corollary 4.1 (Opportunistic Routing): In CRN, the opportunistic routing becomes a promising routing concept for the unreliably links with general nonzero packet-loss probability [96], in which all nodes involved in the route-discovery phase may be applied to the proposed model to determine the best one among neighboring nodes for data relay. Suppose that the source node has to select one neighboring relay node from a set of K candidate numbered relay nodes to route packets. A straightforward selection with high reliability is to select the kth relay path, where $k = \arg_j \max \hat{P}_S^j$ for $j = 1$ to K.

Corollary 4.2 (Trust Estimation): Trust estimation is concerned as the problem of evaluating the trustworthiness of the node based on the history of behavior for some action [21], [97]. If we apply packet transmission to some destination as the action of a neighboring node for trust evaluation, then the success and failure of transmission to some destination are analogous to normal behaviors and misbehaviors of the neighboring node, respectively [98]. The trust measure of the jth neighboring node for relaying the transmission from the source node to some destination node n_D can be defined as $P_{S\to D}^j$. Since $P_{S\to D}^j$ represents the success transmission probability from n_S to n_D through the relaying of the jth neighboring node, the estimation of $P_{S\to D}^j$ thus suggests an approach to estimate the trust. Another interesting application for success probability along a relay path G_j is the trust concatenation of each neighboring pairs along the path, which can be considered as the "trust of path" [21]. Since $P_{S\to D}^j$ represents the success transmission probability from n_S to n_D through path G_j, the estimation of $P_{S\to D}^j$ thus illustrates the estimation of the path trust.

Corollary 4.3 (Congestion Control): The feature that n_D feeds back the collection of observations at one time is suitable for application in end-to-end congestion control. In this application, the transmission through path G_j is regarded as a flow through path G_j, and P_S^j can be regarded as the packet drop rate of the flow. The packet drop rate of a flow implies the successful receiving rate of the flow; thus, P_S^j can generally be considered as the function to measure the degree of congestion of the flow. According to this estimation information, the overall congestion control can be achieved by distributing the packets to the routing path with a lower congestion (a higher success probability).

Remarks: Many active techniques are provided for conventional network tomography problems [40], [88], [89]. Adapted to suitable CRN models, they might be applied in CRN tomography, such as the end-to-end delay inference in [40], and fall into the category of active network-level probing. We also note that *Corollaries* 4.1–4.3 can further be enhanced by adopting more sophisticated statistical inference and networking techniques as future research after successful illustration of active CRN tomography at the multilink (network) level.

V. Conclusion

To statistically infer the required information for CRN operations, we have proposed CRN tomography and established the framework of CRN tomography. CRN tomography can be regarded as a general sensing capability of CRN to obtain the intrinsic parameters and to meet the general needs of CRN operations. In this framework, techniques of CRN tomography can be passive or active, according to the tomography operation, and defined on link- or network-level (parameter) inference, according to the tomography parameters. In this paper, we systematically explore appropriate CRN tomography for smooth CRN operations at the link and network level to open a new dimensional research via statistical inference or learning algorithms. By generally introducing statistic inference in addition to detection and estimation, CRN tomography can further facilitate more advanced features of CRN operations.

Acknowledgment

The authors would like to thank H. Harada, W. Zhuang, and the anonymous reviewers, for their detailed feedback and constructive comments so that the contents and presentation of this paper could be more complete, and S.-Y. Shih for many useful simulation discussions and work.

References

[1] J. Mitola, III, and G. Q. Maguire, Jr., "Cognitive radio: Making software radios more personal," *IEEE Pers. Commun.*, vol. 6, no. 4, pp. 13–18, Aug. 1999.

[2] Fed. Commun. Comm., Spectrum policy task force report, Washington, DC, Nov. 2002.

[3] S. Haykin, "Cognitive radio: Brain-empowered wireless communications," *IEEE J. Sel. Areas Commun.*, vol. 23, no. 2, pp. 201–220, Feb. 2005.

[4] Q. Zhao, S. Geirhofer, L. Tong, and B. M. Sadler, "Opportunistic spectrum access via periodic channel sensing," *IEEE Trans. Signal Process.*, vol. 56, no. 2, pp. 785–796, Feb. 2008.

[5] T. Yucek and H. Arslan, "Spectrum characterization for opportunistic cognitive radio systems," in *Proc. IEEE MILCOM*, Oct. 2006, pp. 23–25.

[6] H. Tang, "Some physical layer issues of wide-band cognitive radio systems," in *Proc. IEEE DySPAN*, Nov. 2005, pp. 151–159.

[7] S.-Y. Lien, C.-C. Tseng, and K.-C. Chen, "Novel rate-distance adaptation of multiple access protocols in cognitive radio," in *Proc. IEEE PIMRC*, Sep. 2007, pp. 1–5.

[8] S. Srinivasa and S. A. Jafar, "How much spectrum sharing is optimal in cognitive radio networks?" *IEEE Trans. Wireless Commun.*, vol. 7, no. 10, pp. 4010–4018, Oct. 2008.

[9] S. Srinivasa and S. A. Jafar, "The throughput potential of cognitive radio: A theoretical perspective," in *Proc. ACSSC*, Oct. 2006, pp. 221–225.

[10] Q. Zhao and B. M. Sadler, "A survey of dynamic spectrum access," *IEEE Signal Process. Mag.*, vol. 24, no. 3, pp. 79–89, May 2007.

[11] C.-H. Huang, Y.-C. Lai, and K.-C. Chen, "Network capacity of cognitive radio relay network," *Phys. Commun.*, vol. 1, no. 2, pp. 112–120, Jun. 2008.

[12] Y. Zhao, L. Morales, J. Gaeddert, K. K. Bae, J.-S. Um, and J. H. Reed, "Applying radio environment maps to cognitive wireless regional area networks," in *Proc. IEEE DySPAN*, Apr. 2007, pp. 115–118.

[13] N. Devroye, P. Mitran, and V. Tarokh, "Cognitive multiple access networks," in *Proc. ISIT*, Sep. 2005, pp. 57–61.

[14] L. Geng, Y.-C. Liang, and F. Chin, "Network coding for wireless ad hoc cognitive radio networks," in *Proc. IEEE PIMRC*, Sep. 2007, pp. 1–5.

[15] S.-Y. Lien, C.-C. Tseng, and K.-C. Chen, "Carrier sensing based multiple access protocols for cognitive radio networks," in *Proc. IEEE ICC*, May 2008, pp. 3208–3214.

[16] S. Delaere and P. Ballon, "Multi-level standardization and business models for cognitive radio: The case of the cognitive pilot channel," in *Proc. IEEE DySPAN*, Oct. 2008, pp. 1–18.

[17] S. Buljore, H. Harada, S. Filin, P. Houze, K. Tsagkaris, O. Holland, K. Nolte, T. Farnham, and V. Ivanov, "Architecture and enablers for optimized radio resource usage in heterogeneous wireless access networks: The IEEE 1900.4 Working Group," *IEEE Commun. Mag.*, vol. 47, no. 1, pp. 122–129, Jan. 2009.

[18] S. Buljore, M. Muck, P. Martigne, P. Houze', H. Harada, K. Ishizu, O. Holland, A. Mihailovic, K. Tsagkaris, O. Sallent, G. Clemo, M. Sooriyabandara, V. Ivanov, K. Nolte, and M. Stametalos, "Introduction to IEEE P1900.4 activities," *IEICE Trans. Commun.*, vol. E91-B, no. 1, pp. 2–9, Sep. 2008.

[19] IST-2003-507995 Project E2R (End-to-End Reconfigurability). [Online]. Available: http://e2r.motlabs.com/

[20] M. Pitchaimani, D. Jeyaraman, and J. Evans, "Adaptive network layer for cognitive radio networks," in *Proc. CROWNCOM*, May 2008, pp. 1–9.

[21] K.-C. Chen, P.-Y. Chen, N. Prasad, Y.-C. Liang, and S. Sun, "Trusted cognitive radio networking," *Wiley Wireless Commun. Mobile Comput.*, vol. 10, no. 4, pp. 467–485, Apr. 2010.

[22] K.-C. Chen, S.-Y. Tu, and C.-K. Yu, "Statistical inference in cognitive radio networks," in *Proc. IEEE ChinaCom*, Aug. 2009, pp. 1–10.

[23] S.-Y. Lien, N. Prasad, K.-C. Chen, and C.-W. Su, "Providing statistical Quality-of-Service guarantee in cognitive radio networks with cooperation," in *Proc. 2nd Int. Workshop CogART*, May 2009, pp. 6–11.

[24] I. F. Akyildiz, W. Y. Lee, M. Vuran, and S. Mohanty, "NeXt generation/dynamic spectrum access/cognitive radio wireless networks: A survey," *Comput. Netw.*, vol. 50, no. 13, pp. 2127–2159, Sep. 2006.

[25] H. Celebi and H. Arslan, "Utilization of location information in cognitive wireless networks," *IEEE Wireless Commun.*, vol. 14, no. 4, pp. 6–13, Aug. 2007.

[26] H. Celebi and H. Arslan, "Enabling location and environment awareness in cognitive radios," *Comput. Commun.*, vol. 31, no. 6, pp. 1114–1125, Apr. 2008.

[27] S. Yarkan and H. Arslan, "Exploiting location awareness toward improved wireless system design in cognitive radio," *IEEE Commun. Mag.*, vol. 46, no. 1, pp. 128–136, Jan. 2008.

[28] H. Celebi and H. Arslan, "Cognitive positioning systems," *IEEE Trans. Wireless Commun.*, vol. 6, no. 12, pp. 4475–4483, Dec. 2007.

[29] H. Celebi and H. Arslan, "Adaptive positioning systems for cognitive radio," in *Proc. IEEE DySpan*, Apr. 2007, pp. 78–84.

[30] S. Gezici, H. Celebi, H. V. Poor, and H. Arslan, "Fundamental limits on time delay estimation in dispersed spectrum cognitive radio systems," *IEEE Trans. Wireless Commun.*, vol. 8, no. 1, pp. 78–83, Jan. 2009.

[31] P. Cordier, P. Houze, S. Jemaa, and O. Simon, "E2R cognitive pilot channel concept," in *Proc. IST Mobile Wireless Summit*, Jun. 2006, vol. 1, pp. 83–99.

[32] J. Perez-Romero, O. Salient, R. Agusti, and L. Giupponi, "A novel on-demand cognitive pilot channel enabling dynamic spectrum allocation," in *Proc. IEEE DySPAN*, Apr. 2007, pp. 46–54.

[33] D. Bourse, R. Agusti, P. Ballon, P. Cordier, S. Delaere, B. Deschamps, D. Grandblaise, A. Lee, P. Martigne, K. Moessner, M. Muck, and O. Sallent, "The E2R II flexible spectrum management (FSM) framework and cognitive pilot channel (CPC) concept—Technical and business analysis and recommendations," IST-E2R II White Paper.

[34] M. Sherman, A. Mody, R. Martinez, C. Rodriguez, and R. Reddy, "IEEE standards supporting cognitive radio and networks, dynamic spectrum access, and coexistence," *IEEE Commun. Mag.*, vol. 46, no. 7, pp. 72–79, Jul. 2008.

[35] J. Yang, Z. Kui, F. Zhiyong, C. Cheng, Z. Ping, and M. Muck, "CPC-assisted network selection strategy," in *Proc. 16th IST Mobile Wireless Commun. Summit*, Jul. 2007, pp. 1–5.

[36] P. Houze, S. B. Jemaa, and P. Cordier, "Common pilot channel for network selection," in *Proc. IEEE VTC—Spring*, May 2006, vol. 1, pp. 67–71.

[37] Y. Vardi, "Network tomography: Estimating source-destination traffic intensities from link data," *J. Amer. Stat. Assoc.*, vol. 91, no. 433, pp. 365–377, Mar. 1996.

[38] S. Geirhofer, L. Tong, and B. M. Sadler, "Dynamic spectrum access in the time domain: Modeling and exploiting white space," *IEEE Commun. Mag.*, vol. 45, no. 5, pp. 66–72, May 2007.

[39] K.-C. Chen and R. Prasad, *Cognitive Radio Networks*. Hoboken, NJ: Wiley, 2009.

[40] A. Coates, A. O. Hero, III, R. Nowak, and B. Yu, "Internet tomography," *IEEE Signal Process. Mag.*, vol. 19, no. 3, pp. 47–65, May 2002.

[41] M. E. Newman, "The structure and function of complex networks," *SIAM Rev.*, vol. 45, no. 2, pp. 167–256, Jun. 2003.

[42] Y.-J. Peng, "Routing challenges for cognitive radio networks," M.S. thesis, Nat. Taiwan Univ., Taipei, Taiwan, Sep. 2008.

[43] D. Cabric, A. Tkachenko, and R. W. Brodersen, "Experimental study of spectrum sensing based on energy detection and network cooperation," in *Proc. TAPAS*, Aug. 2006, paper 12.

[44] Y. Zeng, Y. C. Liang, and R. Zhang, "Blindly combined energy detection for spectrum sensing in cognitive radio," *IEEE Signal Process. Lett.*, vol. 15, pp. 649–652, 2008.

[45] Y. M. Kim, G. Zheng, S. H. Sohn, and J. M. Kim, "An alternative energy detection using sliding window for cognitive radio system," in *Proc. ICACT*, Feb. 2008, vol. 1, pp. 481–485.

[46] B. Shent, L. Huang, C. Zhao, Z. Zhou, and K. Kwak, "Energy detection based spectrum sensing for cognitive radios in noise of uncertain power," in *Proc. ISCIT*, Oct. 2008, pp. 628–633.

[47] W. A. Gardner, "Signal interception: A unifying theoretical framework for feature detection," *IEEE Trans. Commun.*, vol. 36, no. 8, pp. 897–906, Aug. 1988.

[48] P. D. Sutton, K. E. Nolan, and L. E. Doyle, "Cyclostationary signatures in practical cognitive radio applications," *IEEE J. Sel. Areas Commun.*, vol. 26, no. 1, pp. 13–24, Jan. 2008.

[49] Z. Ye, J. Grosspietsch, and G. Memik, "Spectrum sensing using cyclostationary spectrum density for cognitive radios," in *Proc. IEEE Workshop Signal Process. Syst.*, Oct. 2007, pp. 1–6.

[50] H.-S. Chen, W. Gao, and D. G. Daut, "Spectrum sensing using cyclostationary properties and application to IEEE 802.22 WRAN," in *Proc. IEEE GLOBECOM*, Nov. 2007, pp. 3133–3138.

[51] K. Kim, I. A. Akbar, K. K. Bae, J.-S. Um, C. M. Spooner, and J. H. Reed, "Cyclostationary approaches to signal detection and classification in cognitive radio," in *Proc. IEEE DySPAN*, Apr. 2007, pp. 212–215.

[52] D. Cabric, S. M. Mishra, and R. W. Brodersen, "Implementation issues in spectrum sensing for cognitive radios," in *Proc. Asilomar Conf.*, Nov. 2004, pp. 772–776.

[53] M. Hoyhtya, A. Hekkala, M. Katz, and A. Mammela, "Spectrum awareness: Techniques and challenges for active spectrum sensing," in *Cognitive Wireless Networks*, F. H. P. Fitzek and M. D. Katz, Eds. New York: Springer-Verlag, 2007, ch. 18, pp. 353–372.

[54] A. Sahai, R. Tandra, S. M. Mishra, and N. K. Hoven, "Fundamental design tradeoffs in cognitive radio systems," in *Proc. TAPAS*, Aug. 2006, paper 2.

[55] Z. Tian and G. B. Giannakis, "A wavelet approach to wideband spectrum sensing for cognitive radios," in *Proc. CROWNCOM*, Jun. 2006, pp. 1–5.

[56] Y. Youn, H. Jeon, and H. Lee, "Discrete wavelet packet transform based energy detector for cognitive radios," in *Proc. IEEE VTC—Spring*, Apr. 2007, pp. 2641–2645.

[57] Z. Quan, S. Cui, A. H. Sayed, and H. V. Poor, "Wideband spectrum sensing in cognitive radio networks," in *Proc. IEEE ICC*, May 2008, pp. 901–906.

[58] G. Ganesan and Y. Li, "Cooperative spectrum sensing in cognitive radio, Part I: Two user networks," *IEEE Trans. Wireless Commun.*, vol. 6, no. 6, pp. 2204–2213, Jun. 2007.

[59] G. Ganesan and Y. Li, "Cooperative spectrum sensing in cognitive radio, Part II: Multiuser networks," *IEEE Trans. Wireless Commun.*, vol. 6, no. 6, pp. 2214–2222, Jun. 2007.

[60] X. Zheng, L. Cui, J. Chen, Q. Wu, and J. Wang, "Cooperative spectrum sensing in cognitive radio systems," in *Proc. CISP*, May 2008, pp. 262–266.

[61] B. Shen, L. Huang, C. Zhao, K. Kwak, and Z. Zhou, "Weighted cooperative spectrum sensing in cognitive radio networks," in *Proc. ICCIT*, Nov. 2008, pp. 1074–1079.

[62] S. M. Mishra, A. Sahai, and R. W. Broderson, "Cooperative sensing among cognitive radios," in *Proc. IEEE ICC*, Jun. 2006, pp. 1658–1663.
[63] Q. Chen, F. Gao, A. Nallanathan, and Y. Xin, "Improved cooperative spectrum sensing in cognitive radio," in *Proc. IEEE VTC—Spring*, May 2008, pp. 1418–1422.
[64] D. Cabric, "Addressing feasibility of cognitive radios," *IEEE Signal Process. Mag.*, vol. 25, no. 6, pp. 85–93, Nov. 2008.
[65] K.-C. Chen, "Medium access control of wireless LANs for mobile computing," *IEEE Netw.*, vol. 8, no. 5, pp. 50–63, Sep./Oct. 1994.
[66] K.-C. Chen, B. K. Cetin, Y.-C. Peng, N. Prasad, J. Wang, and S. Lee, "Routing for cognitive radio networks consisting of opportunistic links," *Wiley Wireless Commun. Mobile Comput.*, vol. 10, no. 4, pp. 451–466, Apr. 2009.
[67] H. Kim and K. G. Shin, "Efficient discovery of spectrum opportunities with MAC-layer sensing in cognitive radio networks," *IEEE Trans. Mobile Comput.*, vol. 7, no. 5, pp. 533–545, May 2008.
[68] C.-K. Yu and K.-C. Chen, "Multiple systems sensing for cognitive radio networks over Rayleigh fading channel," in *Proc. IEEE VTC—Spring*, May 2008, pp. 1574–1578.
[69] J. M. Mendel, "Tutorial on higher-order statistics (spectra) in signal processing and system theory: Theoretical results and some applications," *Proc. IEEE*, vol. 79, no. 3, pp. 278–305, Mar. 1991.
[70] M. C. Dogan and J. M. Mendel, "Single sensor detection and classification of multiple sources by higher-order spectra," *Proc. Inst. Elect. Eng.—F, Radar Signal Process.*, vol. 140, no. 6, pp. 350–355, Dec. 1993.
[71] Y. Chen, G. Yu, Z. Zhang, H.-H. Chen, and P. Qiu, "On cognitive radio networks with opportunistic power control strategies in fading channels," *IEEE Trans. Wireless Commun.*, vol. 7, no. 7, pp. 2752–2761, Jul. 2008.
[72] A. J. Goldsmith and S.-G. Chua, "Adaptive coded modulation for fading channels," *IEEE Trans. Commun.*, vol. 46, no. 5, pp. 595–602, May 1998.
[73] M. K. Simon and M.-S. Alouini, *Digital Communication Over Fading Channels*, 2nd ed. Hoboken, NJ: Wiley, 2005.
[74] N. Hoven and A. Sahai, "Power scaling for cognitive radio," in *Proc. IWCMC*, Jun. 2005, vol. 1, pp. 250–255.
[75] C.-K. Yu and K.-C. Chen, "Radio resource tomography of cognitive radio networks," in *Proc. IEEE VTC—Spring*, Apr. 2009, pp. 1–5.
[76] S.-Y. Tu and K.-C. Chen, "General spectrum sensing in cognitive radio networks," *IEEE Trans. Inf. Theory*, 2009, submitted for publication. [Online]. Available: http://arxiv.org/abs/0907.2859
[77] S. Hsue and S. Soliman, "Automatic modulation recognition of digitally modulated signals," in *Proc. MILCOM*, Oct. 1989, pp. 645–649.
[78] A. Polydoros and K. Kim, "On the detection and classification of quadrature digital modulations in broad-band noise," *IEEE Trans. Commun.*, vol. 38, no. 8, pp. 1199–1211, Aug. 1990.
[79] E. Azzouz and A. Nandi, "Automatic identification of digital modulation types," *Signal Process.*, vol. 47, no. 1, pp. 55–69, Nov. 1995.
[80] R. J. Lyman, Q. Wang, P. D. Leon, and S. Horan, "Transmission parameter estimation for an autoconfigurable receiver," in *Proc. IEEE Aerosp. Conf.*, Mar. 2004, vol. 2, pp. 1305–1311.
[81] D. R. Pauluzzi and N. C. Beaulieu, "A comparison of SNR estimation techniques for the AWGN channel," *IEEE Trans. Commun.*, vol. 48, no. 10, pp. 1681–1691, Oct. 2000.
[82] M. Mohammad and R. M. Buehrer, "On the impact of SNR estimation error on adaptive modulation," *IEEE Commun. Lett.*, vol. 9, no. 6, pp. 490–492, Jun. 2005.
[83] R. Zhang and Y.-C. Liang, "Exploiting hidden power-feedback loops for cognitive radio," in *Proc. IEEE DySPAN*, Oct. 2008, pp. 1–5.
[84] E. W. Knightly and N. B. Shroff, "Admission control for statistical QoS: Theory and practice," *IEEE Netw.*, vol. 13, no. 2, pp. 20–29, Mar./Apr. 1999.
[85] R. Caceres, N. Duffield, J. Horowitz, and D. Towsley, "Multicast based inference of network internal loss characteristics," *IEEE Trans. Inf. Theory*, vol. 45, no. 7, pp. 2462–2480, Nov. 1999.
[86] M. Coates and R. Nowak, "Network loss inference using unicast end-to-end measurement," in *Proc. ITC Semin. IP Traffic, Meas. Modelling*, Sep. 2000, pp. 28:1–28:9.
[87] G. Liang and B. Yu, "Maximum pseudo likelihood estimation in network tomography," *IEEE Trans. Signal Process.*, vol. 51, no. 8, pp. 2043–2053, Aug. 2003.
[88] M. G. Rabbat, M. J. Coates, and R. D. Nowak, "Multiple-source Internet tomography," *IEEE J. Sel. Areas Commun.*, vol. 24, no. 12, pp. 2221–2234, Dec. 2006.
[89] M. G. Rabbat, M. A. T. Figueiredo, and R. D. Nowak, "Network inference from co-occurrences," *IEEE Trans. Inf. Theory*, vol. 54, no. 9, pp. 4053–4068, Sep. 2008.
[90] M. Abramowitz and I. A. Stegun, *Handbook of Mathematical Functions With Formulas, Graphs, and Mathematical Tables*. New York: Dover, 1965.
[91] K. Raman, The Laplace Rule of Succession Under a General Prior, May 2000. [Online]. Available: http://interstat.statjournals.net/YEAR/2000/articles/0006001.pdf
[92] W. Chang, "Preemptive priority queue," *Oper. Res.*, vol. 13, no. 5, pp. 820–827, Sep. 1965.
[93] D. P. Heyman and M. J. Sobel, *Stochastic Models in Operations Research, Vol. I: Stochastic Processes and Operating Characteristics*. New York: McGraw-Hill, 1982.
[94] M. R. Spiegel, "Correlation theory," in *Theory and Problems of Probability and Statistics*, 2nd ed. New York: McGraw-Hill, 1992, ch. 14, pp. 294–323.
[95] C. Leong, Z. Weihua, C. Yu, and W. Lei, "Call admission control for integrated on/off voice and best-effort data services in mobile cellular communications," *IEEE Trans. Commun.*, vol. 52, no. 5, pp. 778–790, May 2004.
[96] S. Biswas and R. Morris, "Opportunistic routing in multi-hop wireless networks," *ACM SIGCOMM Comput. Commun. Rev.*, vol. 34, no. 1, pp. 69–74, Jan. 2004.
[97] A. A. Rahman and S. Halles, "A distributed trust model," in *Proc. Workshop New Security Paradigms*, Sep. 1997, pp. 48–60.
[98] L. Mui, M. Mohtashemi, and A. Halberstadt, "A computational model of trust and reputation," in *Proc. HICSS*, Jan. 2002, pp. 2431–2439.

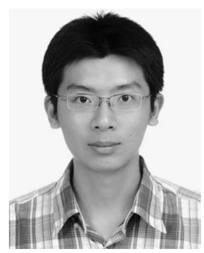

Chung-Kai Yu (S'08–M'09) received the B.S. degree in electrical engineering and the M.S. degree in communication engineering from National Taiwan University, Taipei, Taiwan, in 2006 and 2008, respectively.

He is currently with the Graduate Institute of Communication Engineering, National Taiwan University. His research interests include cognitive radio networks, statistical signal processing, and wireless communication systems.

Kwang-Cheng Chen (F'07) received B.S. degree from the National Taiwan University, Taipei, Taiwan, in 1983 and the M.S. and Ph.D. degrees from the University of Maryland, College Park, in 1987 and 1989, all in electrical engineering.

From 1987 to 1998, he was with SSE, COMSAT, the IBM Thomas J. Watson Research Center, and National Tsing Hua University, Hsinchu, Taiwan, working on mobile communications and networks. Since 1998, he has been with National Taiwan University, where he is the Distinguished Professor and Director for the Graduate Institute of Communication Engineering and Director for the Communication Research Center. His research interests include wireless communications and network science.

Dr. Chen has actively been involved with the technical organizations of numerous leading IEEE conferences, including as the Technical Program Committee (TPC) Chair of the 1996 IEEE International Symposium on Personal, Indoor, and Mobile Radio Communications, TPC co-chair for the 2002 IEEE Globecom, General Co-Chair for the 2007 IEEE Mobile WiMAX Symposium, Orlando, FL, the 2009 IEEE Mobile WiMAX Symposium, Napa Valley, CA, the IEEE 2010 Spring Vehicular Technology Conference, and the 2010 IEEE Workshop on Social Networks. He has served editorships with many IEEE and international journals and served in various positions within the IEEE. He also actively participates in various wireless international standards. He has authored and co-authored over 200 technical papers and has 18 granted U.S. patents. He co-edited (with R. DeMarca) the book *Mobile WiMAX* (Wiley 2008) and authored the book *Principles of Communications* (River, 2009), and co-authoed (with R. Prasad) another book *Cognitive Radio Networks* (Wiley 2009). He has received numerous awards and honors.

Shin-Ming Cheng (S'05–M'07) received the B.S. and Ph.D. degrees in computer science and information engineering from National Taiwan University, Taipei, Taiwan, in 2000 and 2007, respectively.

In 2007, he joined the Department of Electrical Engineering, National Taiwan University, as a Postdoctoral Researcher. His research interests include network security, performance modeling, and cognitive radio networks.